

T.46

A
THESIS ON

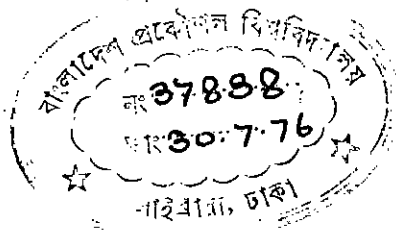
"AN INVESTIGATION INTO A CLASS OF TRANSISTOR INTERSTAGE
NETWORKS FOR BANDPASS CHARACTERISTICS".

SUBMITTED TO

THE DEPARTMENT OF ELECTRICAL ENGINEERING,
BANGLADESH UNIVERSITY OF ENGINEERING & TECHNOLOGY, DACCA,

IN PARTIAL FULFILMENT OF THE REQUIREMENT OF

THE DEGREE OF
MASTER OF SCIENCE (ENGG.)
IN ELECTRICAL ENGINEERING



BY

MD. ABUL HANNAN MAZUMDER
DEPARTMENT OF ELECTRICAL ENGINEERING,
BANGLADESH UNIVERSITY OF ENGINEERING & TECHNOLOGY,
DACCA.

JUNE 1976.



#37838#

CERTIFICATE

THIS IS TO CERTIFY THAT THIS WORK HAS DONE
BY ME AND IT HAS NOT BEEN SUBMITTED ELSEWHERE FOR
THE AWARD OF ANY DEGREE OR DIPLOMA OR FOR PUBLICATION.

Countersigned

Solaiman Ahmad
(Supervisor) 17/7/76

Md. Abdul Mannan Mazumder
Signature of the Candidate. 17/7/76

T. 46

ACCEPTED AS SATISFACTORY FOR PARTIAL FULFILMENT
OF THE REQUIREMENTS FOR THE DEGREE OF M.Sc. (ENGG.)
IN ELECTRICAL ENGINEERING.

EXAMINERS:

- (i) S. Srinivasan Mahalingam
- (ii) Madhavan 17/7/76
- (iii) A. Srinivasan 17/7/76
- (iv) A. M. Srinivasan 17/7/76
- (v) Srinivasan 17/7/76

ACKNOWLEDGEMENT

The author expresses his indebtedness and deep sense of gratitude to his supervisor Dr. Solaimanul Mahdi, Professor of Electrical Engineering, Bangladesh University of Engineering and Technology, Dacca, for his constant encouragement and valuable guidance throughout the course of this work.

The author also wishes to express his sincere gratitude and thanks to Dr. A. N. Zaborul Haq, Professor and Head of the Department of Electrical Engineering, Bangladesh University of Engineering and Technology, Dacca, for the facilities provided in the department.

Thanks are due to the authorities and the members of the staff of Computer Division of the Bureau of Statistics, the Govt. of the People's Republic of Bangladesh, whose cooperation made it possible for this study to be completed.

Valuable help received from the members of the staff of the Department of Electrical Engineering, Bangladesh University of Engineering and Technology, Dacca, are highly appreciated and also thankfully acknowledged.

ABSTRACT

Two methods of synthesizing interstage networks for a multistage transistorized filter to achieve bandpass response of desired specification have been given. The first method deals with synthesizing each interstage that must realize a certain number of poles and zeros of the over-all transfer function that achieves the prescribed response. The second one deals with synthesizing an interstage of pre-selected configuration to achieve the prescribed response.

Using frequency transformation, the bandpass response specifications were converted into the corresponding lowpass specifications. Chebyshev approximation was used to obtain a rational realizable transfer function satisfying the lowpass specifications. Applying lowpass to bandpass transformation, transfer function that met bandpass specifications was found. The transmission poles and zeros were divided amongst the interstages determining their number and configuration.

When each interstage was designed to achieve one pair of poles and two zeros, a single tuned circuit resulted for each interstage.

When double tuned circuit was selected for the configuration of the interstages, it was found that although the composite circuit was capable of realizing the desired transmission poles, its transmission zeros were not divided equally between the origin and the infinity as the desired zeros were. Since the location of zeros were fixed for the selected configuration, the pole locations were adjusted to have symmetrical response about the centre frequency and to keep passband response within tolerable limit.

Two examples, one for each method, of designing transistorized bandpass amplifier were furnished, prototypes were constructed and their measured performances were as expected.

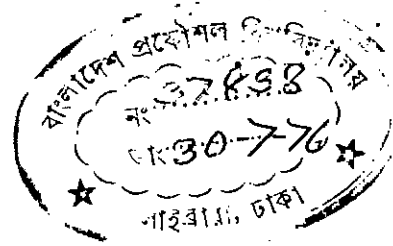
CONTENTS

		<u>Page</u>
CHAPTER-1	INTRODUCTION	1
CHAPTER-2	APPROXIMATION	5
	2.1 BUTTERWORTH POLYNOMIALS IN APPROXIMATION	6
	2.2 CHEBYSHEV POLYNOMIALS IN APPROXIMATION	9
	2.3 FREQUENCY TRANSFORMATION FROM LOWPASS TO BANDPASS	15
	2.4 EXAMPLE OF FREQUENCY TRANSFORMATION	17
CHAPTER-3	A GENERAL FILTER CIRCUIT	20
	3.1 GENERAL CONSIDERATION	20
	3.2 GENERAL ANALYSIS OF AN ACTIVE FILTER CIRCUIT	21
	3.3 SYNTHESIS OF THE TYPICAL i TH INTERSTAGE	
	3.4 REALIZATION OF PRESCRIBED RESPONSE WITH SELECTED RATIONAL FUNCTION	24
	3.5 REALIZATION OF PRESCRIBED RESPONSE WITH SELECTED CONFIGURATION	30
	3.5.1 METHODS FOR SOLUTION OF EQN. (3.32)	34
CHAPTER-4	ACTIVE FILTER DESIGN WITH SINGLE TUNED INTERSTAGES	38
	4.1 SPECIFICATION	38
	4.2 DETERMINATION OF BANDPASS POLES & ZEROS	40
	4.3 DETAILED CONSIDERATION OF A TYPICAL STAGE	40
	4.4 DESIGN FOR A SPECIFIED QUIESCENT POINT	43
	4.5 DETERMINATION OF VALUES OF PARAMETERS FOR EACH INTERSTAGE	44

	<u>PAGE</u>
4.6 COMPARISON OF MEASURED FREQUENCY RESPONSE CHARACTERISTICS WITH THEORETICAL CHARACTERISTIC	48
CHAPTER-5 ACTIVE FILTER DESIGN WITH DOUBLE TUNED INTERSTAGE	49
5.1 SPECIFICATION	49
5.2 DETERMINATION OF BANDPASS POLES & ZEROS	50
5.3 DETAILED CONSIDERATION OF A TYPICAL STAGE	51
5.4 ADJUSTMENT OF POLE LOCATIONS FOR SYMME- TRICAL FREQUENCY RESPONSE CHARACTERISTIC	54
5.5 DETERMINATION OF VALUES OF PARAMETER FOR EACH INTERSTAGE	55
5.6 COMPARISON OF MEASURED FREQUENCY RESPONSE CHARACTERISTIC WITH THEORE- TICAL CHARACTERISTIC	60
CHAPTER-6 SUMMARY, CONCLUSION AND FURTHER WORK	61
APPENDICES:	
APPENDIX-A MEASUREMENT OF h-PARAMETERS	64
APPENDIX-B DETERMINATION OF BANDPASS POLES	72
APPENDIX-C DETERMINATION OF THE FREQUENCY RESPONSE OF A CHEBYSHEV ACTIVE BANDPASS FILTER	73
APPENDIX-D DETERMINATION OF THE POLE LOCATIONS FOR SYMMETRICAL FREQUENCY RESPONSE IN DOUBLE TUNED NETWORK	74
APPENDIX-E DETERMINATION OF THE PARAMETERS OF EACH INTERSTAGE OF THE DOUBLE TUNED FILTER	75
REFERENCES	76

T. 46

CHAPTER - 1



INTRODUCTION

Electronic circuits often deal with signals of different frequencies. For example, the signal input to an audio circuit may have both high and low audio frequencies; an r-f circuit can have a wide range of radio frequencies in its input; the audio detector in a radio has both radio frequencies and audio frequencies in the output.

In such applications where the signal has components of frequencies, it is usually necessary either to favour or to reject one frequency or a group of frequencies.

The frequency characteristics of certain types of networks can be employed to separate waves of different frequencies. The separation may be effected primarily for the purpose of selecting a desired band of frequencies or for the purpose of rejecting an undesired band. Selected bands are called pass or transmission bands, and rejected bands are called stop or attenuation bands. Any network which possesses definite properties of frequency discrimination and which is capable of separating electric waves of different frequencies is called an electric wave filter or, a filter¹.

In terms of their function, filters can be classified as either low-pass or high pass. A low-pass filter allows the lower-frequency components of the applied signal to develop output across the load while the higher frequency components are attenuated or reduced at the output. A high-pass filter does the opposite, allowing the higher-frequency components of the applied signal to develop across the load.

In order to make the filtering more selective in terms of which frequencies are passed to produce output voltage across the load, filter

Circuits generally combine inductance and capacitance. Since inductive reactance increases with higher frequencies, while capacitive reactance decreases, the two opposite effects improve the filtering action. With combination of L and C, filters are named to correspond to the circuit configuration. The most common types are the L, T and Π arrangements.

A high-pass filter can be combined with a low-pass filter to pass the band of frequencies that are not stopped by either circuit. In such case, the combination is called a band-pass filter.

Tuned circuits provide a convenient method of filtering a band of radio frequencies, because relatively small values of L and C are necessary for resonance. A tuned circuit provides filtering action by means of its maximum response at the resonant frequency. The width of the band of frequencies affected by resonance depends on the quality factor² Q of the tuned circuit, higher Q providing narrower bandwidth. Such filters are called band-stop or band-pass filter.

There are two competitive methods of filter design. One was originated by Zobel and is well known as the image-parameter method³. The second was originated by Norton and Bennett and is known as the exact method, Polynomial method, or insertion loss method⁴.

The image-parameter theory filter is based on the properties of transmission lines. A simple network with lumped components is described in terms of this continuous structure. Several of such elementary networks with equal characteristic terminal impedances, connected together to produce a chain of ladder networks, will possess a transmission constant equal to the sum of all the individual transmission constants of the elementary sections.

The image-parameter method seems to be in disrepute among the network theorists partially because of the cut-and-try method that is involved and partly because of the restricted freedom of design.

Polynomial method deals directly with effective parameters and provides an elegant solution to the approximation problem. This method involves the determination of an approximate rational function⁵ to represent the driving-point or the transfer impedance of the network the frequency response of which approximates the desired one. Solution to an appropriate approximation problem is thus first step in the design procedure. It yields the rational function representation for the desired response characteristic of the network. The second step involves the realization of this rational function into a network of selected configuration. Naturally the rational function should be such that it is realizable. The approximation problem is thus concerned with the construction of a rational function fulfilling, on the one hand, the appropriate realizability conditions, and on the other, the demand of the given data regarding the performance characteristics of the desired network.

When a filter circuit contains active elements transistor, for example, it is called an active filter⁶. Active filter configuration may vary widely. However, many of these filters may be looked upon as consisting of a chain of active elements between each pair of which a passive circuit, called "interstage network"⁷, has been interposed.

This study is limited to those active circuit configurations that admit of separation into a number of sections in such a way that the total transfer function is given by the product of the individual transfer functions of the sections, and aims at achieving prescribed bandpass frequency response for the filter.

Nature of the interstage networks and the circuit elements that model the active element, determine the shape of the over-all characteristics of the filters. The interstage can be synthesized for any specified filter characteristics. Such general considerations will lead to networks of varying configurations. Limiting filter transfer function to a class will restrict the networks also to certain configurations.

The transfer functions of the interstage networks must bear a definite relation with the over-all transfer function of the filter circuit, because the

interstage networks are to be used to realize the zeros and the poles of the over-all transfer function that achieve the prescribed response.

Since the poles and zeros of the transfer function of the filter are determined to satisfy the given specifications, finding the transfer function of the individual interstages depends on their respective position with respect to the total configuration of the filter and on their number. The chosen filter configuration is such that the product of the transfer functions of the interstages gives the over-all transfer function. Thus several of the critical frequencies of the transfer functions can be assigned to an interstage for realization, subject to the condition of realizability. The way the poles and zeros of the transfer function of the filter are divided amongst the interstages will determine their number and configuration. If however the configuration of the interstage is already selected, so that the nature of location and the number of the poles and zeros of its transfer function are fixed, the critical frequencies of the over-all transfer function must be compatible with these in addition to satisfying the design specification.

The parameters of each interstage depend on the positions of the poles and the zeros that have been assigned to this stage for realization.

CHAPTER- 2

APPROXIMATION

In many applications, such as in active and passive electric filters, it is required that the magnitude of the transfer function be ideally constant within a certain desired frequency range, called the passband, and ideally zero over the rest of the frequencies referred to as the stopband. Such an ideal magnitude response for low-pass networks is shown in fig.2.1.

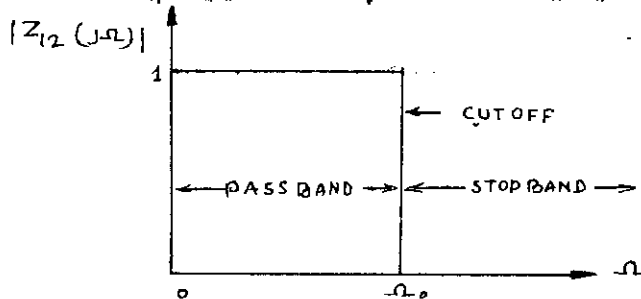


Fig.2.1 : Ideal Low-pass filter characteristic.

The transfer function, described graphically in fig.2.1, is not physically realizable; therefore one can only attempt to find rational functions which approximate such behaviour. In some other applications linear variation of the angle of magnitude function with frequency may be desired. Here again, a rational function fails to realize such ideal behaviour and one must resort to approximation.

A number of different methods can be adopted to approximate ideal characteristic shown in fig.2.1, namely:

- (1) by trail and error-which usually leads to an error curve of a generally oscillatory nature.
- (2) by minimization of the mean-square error- which gives more or less the same type of error function.
- (3) by Taylor approximation-which gives substantially zero error in the vicinity of the point of maximal approximation.

(4) by Butterworth approximation which gives maximally flat response and falls less sharply outside the approximation band.

(5) by Chebyshev approximation - which gives equiripple response in the approximation band and falls rapidly outside the approximation band.

One of the above mentioned methods can be used to approximate the ideal characteristics. But in practice, requirements are such that the greater the sharpness outside approximation band the better the performance of the system to which the filter is incorporated. Thus by using the last two methods, we can have better results compared with the other methods.

In this chapter, we shall discuss only the Butterworth and the Chebyshev approximation.

The approximation problem to be solved may be looked upon as that of approximating a constant over a finite range of frequencies. To introduce this concept, we shall consider the ideal magnitude characteristic of the low-pass filter. Confining attention to the low-pass filter is not so restrictive as it appears at first glance, since by using suitable frequency transformation we can convert the low-pass magnitude approximation to a high-pass, bandpass or band elimination characteristic.

2.1 Butterworth Polynomials in approximations

Consider the ideal magnitude characteristic of a low-pass filter shown in fig.2.1, where the magnitude of the transfer impedance is plotted against positive values of the real frequency. In this plot all signals with frequencies in the pass-band $0 \leq \Omega \leq \Omega_c$ are transmitted without loss, whereas inputs with frequencies $\Omega > \Omega_c$ yield zero output. It is known that such a characteristic (because it equals zero over a non-zero range of frequencies) is unrealizable by a physical network, so that it becomes necessary to approximate it.

The function being looked for must approximate a constant in each of the two ranges: unity in the range $0 \leq \Omega \leq \Omega_c$ and zero for $\Omega > \Omega_c$. Thus if the function

$$|Z_{12}(j\Omega)| = \frac{1}{[1 + A_n(\Omega)]^{1/2}} \dots\dots\dots(2.1)$$

is used, it is necessary that

$$A_n(\Omega) \ll 1, \quad 0 \leq \Omega \leq \Omega_0$$

$$A_n(\Omega) \gg 1, \quad \Omega > \Omega_0$$

Butterworth suggested that $A_n(\Omega^2) = \Omega^{2n}$ be used as an approximation. The eqn.(2.1) thus becomes

$$|Z_{12}(j\Omega)| = \frac{1}{[1 + \Omega^{2n}]^{1/2}} \dots\dots\dots(2.2)$$

The response function represented by eqn.(2.2) is known as the nth-order Butterworth or maximally flat⁶ low-pass response and is an approximation to the ideal response of fig.2-1. The nature of the approximation function is seen from two observations:

(1) From the binomial series expansion of expression $\frac{1}{[1 + \Omega^{2n}]^{1/2}}$, we see that near $\Omega = 0$

$$\frac{1}{[1 + \Omega^{2n}]^{1/2}} = (1 + \Omega^{2n})^{-1/2} = 1 - \frac{1}{2} \Omega^{2n} + \frac{3}{8} \Omega^{4n} - \frac{5}{16} \Omega^{6n} + \dots$$

and from this expression the first $(2n-1)$ derivatives are zero at $\Omega = 0$

(2) The magnitude $|Z_{12}(j\Omega)| = 0.707$ for all n.

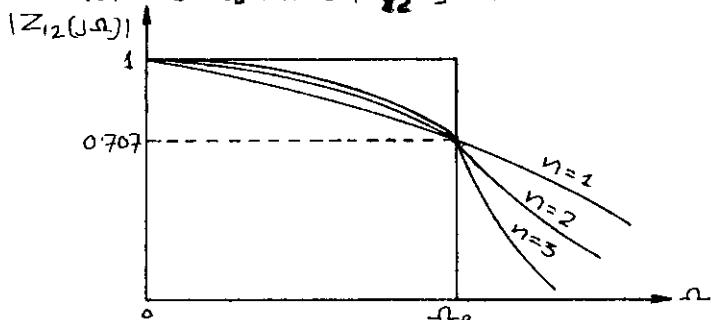


Fig. 2.2: Butterworth responses $\frac{1}{[1 + \Omega^{2n}]^{1/2}}$ for n = 1, 2, 3

The magnitude of $Z_{12}(j\Omega)$ plotted against frequency Ω is shown in fig.2.2 for n = 1, 2, 3. It is observed that the characteristic is monotonic in both the

passband and stopband. It is also clear that the higher the value of n , the greater the degree of maximal flatness possible.

The poles of the Butterworth function are given by the roots of

$$1 + (-s^2)^n = 0 \quad \dots\dots(2.3)$$

The roots of eqn.(2.3) are given by

$$s_k = e^{j \frac{2k + n - 1}{n} \frac{\pi}{2}}, \quad k = 1, 2, \dots\dots 2n \quad - (2.4).$$

The poles so obtained are located on a unit circle in the s -plane and have symmetry with respect to both the real and the imaginary axes. Pole locations for $n=1$, $n=2$, and $n=3$ are shown in fig. 2.3.

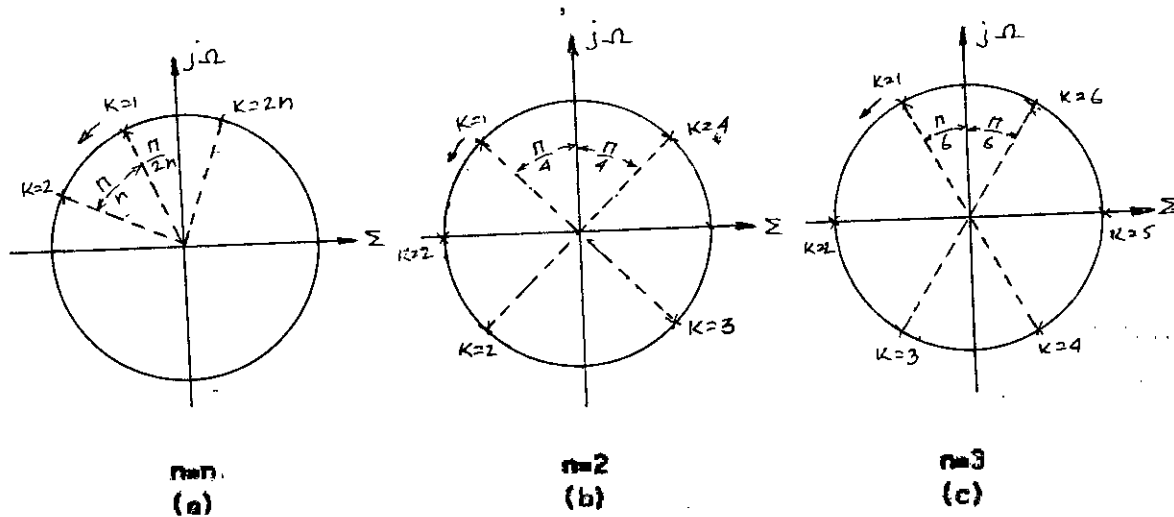


Fig.2.3: Butterworth pole locations for $n=1$, $n=2$ and $n=3$.

From eqn.(2.3) , we have

$$z_{12}(s) z_{12}(-s) \Big|_{s=j\Omega} = |z_{12}(j\Omega)|^2 = \frac{1}{1 + \Omega^{2n}} \quad - (2.5)$$

The polynomial $B_n(s)$ of degree n is now formed such that it possesses all the left half plane critical frequencies indicated in fig. 2.3(a). The polynomial $B_n(-s)$ has therefore, the remaining critical frequencies of fig.2.3(a), which are

in the right half plane.

Therefore,

$$\frac{1}{B_n(s) B_n(-s)} = \frac{1}{1 + (-s^2)^n} = \frac{1}{1 + \Omega^{2n}} \quad \dots(2.6) \quad \left|_{\Omega = \frac{s}{j}}$$

It then follows from eqn.(2.5) and eqn.(2.6) that

$$Z_{12}(s) = \frac{1}{B_n(s)}$$

Thus $Z_{12}(s)$ is an all-pole rational function, its poles being the s 's as those of the left half plane poles of Butterworth polynomial.

2.2 Chebyshev Polynomials in approximation:

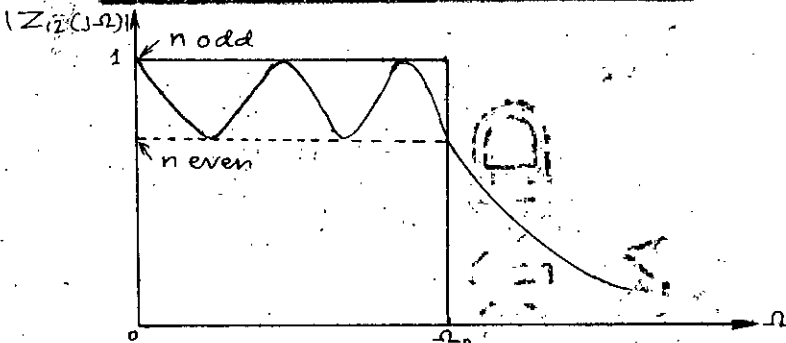


Fig.2.4 : An approximation with Equi-Ripple in the Passband.

An approximation that gives a more uniform coverage throughout the passband is the oscillating one shown in fig. 2.4. The magnitude response varies between equal maximum and equal minimum values in the passband and decreases monotonically outside it, the plot is thus said to have an equal-ripple⁹ (or equi-ripple) character in the passband. Such a characteristic with equal peaks and valleys may be obtained by the use of Chebyshev polynomials.

Chebyshev polynomials $C_n(\Omega)$ are defined in terms of the real variable Ω by the equation:

$$C_n(\Omega) = \cos(n \cos^{-1} \Omega) \dots\dots\dots(2.7)$$

where n is a positive integer denoting the order of the polynomial $C_n(\Omega)$.

The expression $\cos(n \cos^{-1} \Omega)$ may easily be put into recognizable polynomial as follows:

Let

$$\phi = \cos^{-1} \Omega$$

so that $\cos \phi = \Omega$

$$\text{Therefore } C_n(\Omega) = \cos n\phi \dots\dots\dots(2.8)$$

Substituting this equation into the trigonometrical identity

$$\cos(n+1)\phi = 2 \cos n\phi \cos \phi - \cos(n-1)\phi \dots\dots(2.9)$$

We have the recurrence formula

$$C_{n+1}(\Omega) = 2\Omega C_n(\Omega) - C_{n-1}(\Omega) \dots\dots(2.10)$$

Since $C_0(\Omega) = 1$ and $C_1(\Omega) = \Omega$ from eqn.(2.7), other Chebyahav polynomials may be found by using eqn.(2.10).

For $|\Omega| > 1$, $\cos^{-1} \Omega = j \cosh^{-1} \Omega$, so that eqn.(2.7) becomes

$$C_n(\Omega) = \cosh(n \cosh^{-1} \Omega) \dots\dots(2.11)$$

Several useful properties of Chebyahav polynomials are shown in fig.2.5.

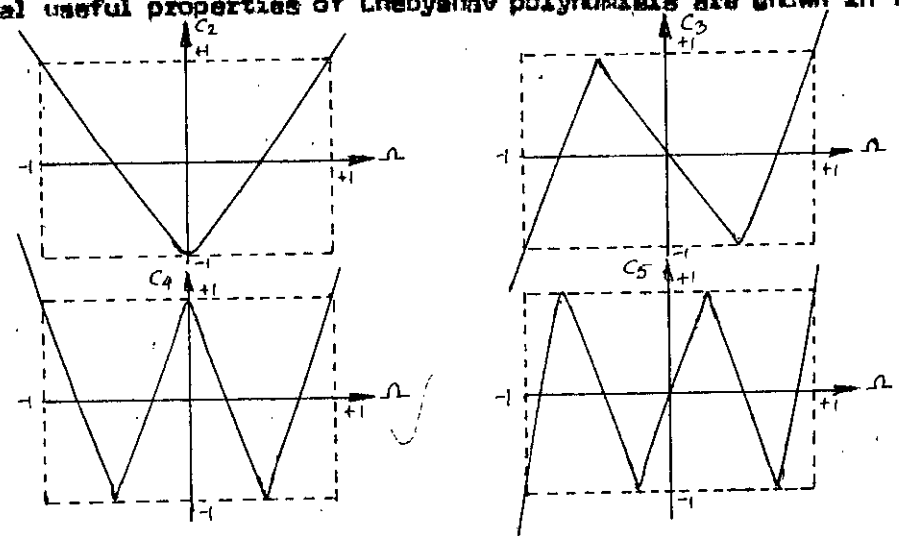


Fig.2.5 : Sketches of Chebyahav Polynomials C_n for $n = 2, 3, 4, 5$.

The zeros of the polynomials are all located in the interval $-1 \leq \Omega \leq 1$ and within this interval the maximum value attained is +1, the minimum value -1 ; i.e.,

$$|C_n| \leq 1 \text{ for } -1 \leq \Omega \leq 1$$

Outside of this interval, the magnitude of the polynomial becomes very large in comparison with unity.

Since the polynomials take on negative as well as positive values with maximum absolute value of unity in the passband $-1 \leq \Omega \leq 1$, they are not suitable by themselves to approximate a magnitude function with a value of unity in the passband. We shall therefore use a ripple factor ϵ as a multiplier of the square of the Chebyshev Polynomial in order to limit the amplitude of its oscillation. To obtain the even function that is required for the representation of a magnitude characteristic, we could use the square of a Chebyshev Polynomial or Polynomials of order $2n$ for $n = 1, 2, 3, \dots$

Thus a function to approximate the ideal lowpass characteristic of fig. 2-1 has the squared magnitude form

$$|Z_{12}(j\Omega)|^2 = \frac{1}{1 + \epsilon^2 C_n^2(\Omega)} \quad \dots\dots\dots(2.12)$$

The response of eqn.(2.12) is shown in fig. 2.4. From the curves of fig. 2.5, we have

$$\begin{aligned} C_n(0) &= (-1)^{n/2} \text{ and } C_n(\pm 1) = 1, \quad n \text{ even.} \\ C_n(0) &= 0 \text{ and } C_n(\pm 1) = \pm 1, \quad n \text{ odd} \quad \dots\dots\dots(2.13) \end{aligned}$$

The maximum value of the response in fig. 2-4 is unity and this value corresponds to points of Ω where $C_n(\Omega) = 0$. The maximum value of the response in the passband is $\frac{1}{\sqrt{1+\epsilon^2}}$, occurring when $|C_n(\Omega)| = 1$. Thus $|Z_{12}(0)|$ is unity for all odd n and $\frac{1}{\sqrt{1+\epsilon^2}}$ for all even n . Similarly $|Z_{12}(1)| = \frac{1}{\sqrt{1+\epsilon^2}}$ for all n as shown in fig. 2.4. The ripple width i.e. difference of maxima and minima in the passband may be approximated for small ϵ by

$$1 - \frac{1}{\sqrt{1+\epsilon^2}} = \frac{\epsilon^2}{2}, \quad \dots\dots(2.14)$$

For large values of Ω , $|Z_{12}(j\Omega)|$ becomes

$$|Z_{12}(j\Omega)| = \frac{1}{\epsilon C_n(\Omega)}, \quad \Omega \gg 1 \quad \dots\dots(2.15)$$

From the last two equations, we can conclude that the permissible ripple width fixes ϵ and the rate of decrease of the magnitude function in the stopband fixes n .

The poles of the Chebyshev function of eqn.(2.12) are given by the roots of

$$1 + \epsilon^2 C_n^2(\Omega) = 0 \quad \dots\dots\dots(2.16)$$

Then the poles of interest occur when

$$C_n(\Omega) = \pm \frac{j}{\epsilon} \quad \dots\dots\dots(2.17)$$

Let $\Omega = \cos z$ where $z = u + jv$, then eqn.(2.17) becomes

$$C_n(\Omega) = \cos(ncos^{-1}\Omega) = \cos nz = \cos nu \cosh nv - j \sin nu \sinh nv = \pm \frac{j}{\epsilon} \dots\dots(2.18)$$

This equation is satisfied when

$$\cos nu \cosh nv = 0 \quad \dots\dots\dots(2.19) \text{ and}$$

$$\sin nu \sinh nv = \pm \frac{1}{\epsilon} \quad \dots\dots\dots(2.20)$$

Since $\cosh nv \neq 0$, from eqn.(2.19), we have $\cos nu = 0$

$$\text{or, } u = \frac{1}{n} - (2k-1) \frac{\pi}{2}, \quad k = 1, 2, \dots, 2n \quad \dots\dots(2.21)$$

At these values of u , $\sin nu = \pm 1$, so that from eqn.(2.20),

$$nv = \sinh^{-1} \frac{1}{\epsilon} \quad \dots\dots\dots(2.22)$$

We define the value of u satisfying this equation to be a , ϵ ; that

$$a = \frac{1}{n} \sinh^{-1} \frac{1}{\epsilon} \quad \dots\dots\dots(2.23)$$

The pole positions in the s -plane are

$$S = j\Omega = j \cos \alpha = j \cos(u + jv) = j \cos \frac{\pi}{2n} (2k-1) + ja \quad (2.24)$$

$k = 1, 2, \dots, 2n$

Expanding this equation, the pole locations $S_k = -\Sigma_k + j\Omega_k$ are found to be

$$\Sigma_k = \pm \sinh a \sin \left(\frac{2k-1}{n} \right) \frac{\pi}{2}, \quad k = 1, 2, \dots, 2n \quad \dots (2.25)$$

and $\Omega_k = \pm \cosh a \cos \left(\frac{2k-1}{n} \right) \frac{\pi}{2}$

Squaring these expressions and adding yield

$$\frac{\Sigma_k^2}{\sinh^2 a} + \frac{\Omega_k^2}{\cosh^2 a} = 1 \quad \dots (2.26)$$

This is the equation of an ellipse. The major semi-axis of the ellipse has the value $\cosh a$, the minor semi-axis is $\sinh a$ and the foci are located at $\Omega = \pm 1$.

Consider the frequency $\Omega_a = \cosh a$ at which this ellipse crosses the imaginary axis of the s-plane. At this frequency

$$C_n(\Omega_a) = \cosh^n \cosh^{-1} \cosh a = \cosh^n a \quad \dots (2.27)$$

But $na = \sinh^{-1} \frac{1}{\epsilon} = \cosh^{-1} \left(1 + \frac{\epsilon^2}{2} \right)^{1/2} \quad \dots (2.28)$

$$C_n(\Omega_a) = \left(1 + \frac{1}{\epsilon^2} \right)^{n/4} \quad \dots (2.29)$$

Then the magnitude response $|Z_{12}|$ has the value

$$|Z_{12}(j \cosh a)| = \frac{1}{[1 + \epsilon^2 C_n^2(\cosh a)]^{1/2}} = \frac{1}{(2 + \epsilon^2)^{1/2}} \quad \dots (2.30)$$

for $\epsilon \ll 1$

$$|Z_{12}(j \cosh a)| = \frac{1}{\sqrt{2}} = 0.707 \quad \dots (2.31)$$

which is the half power or the cut off frequency of the Butterworth response. So we can compare the Butterworth response at frequency $\Omega = 1$ with Chebyshev response at frequency $\Omega = \cosh a$.

Normalizing the frequency of the Chebyshev response by the factor $\cosh a$, then the eqn. (2.25) becomes,

$$\Sigma'_k = \pm \tanh \sigma \sin \left(\frac{2k-1}{n} \right) \frac{\pi}{2}$$

$$\text{and } \Omega'_k = \cos \left(\frac{2k-1}{n} \right) \frac{\pi}{2} \dots\dots(2.32)$$

The pole locations for Butterworth case with n even,

$$\Sigma_k = \cos \left(\frac{2k-1}{n} \right) \frac{\pi}{2}, \quad K = 1, 2, \dots, 2n.$$

$$\text{and } \Omega_k = \sin \left(\frac{2k-1}{n} \right) \frac{\pi}{2} \quad K = 1, 2, \dots, 2n \quad \dots\dots(2.33)$$

Comparing eqns(2.32) and (2.33), we can say that poles are same except that the sine and cosine terms are interchanged with different multipliers.

The pole locations for the various K found from eqn. (2.33) are shown in fig.2.6. The corresponding Chebyshev pole locations are shown in fig. 2.7 with different starting point and a different direction of rotation.

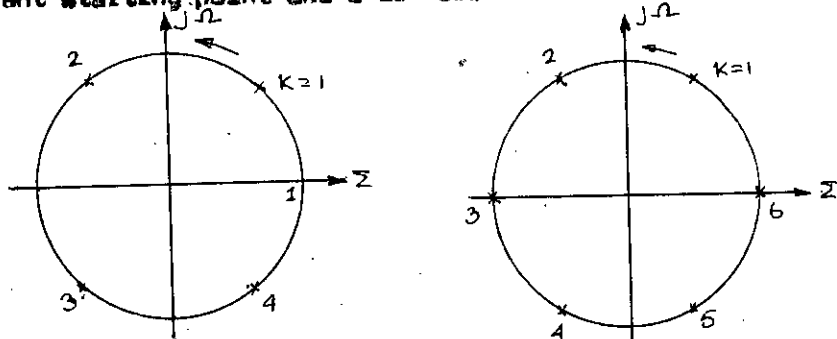


Fig. 2.6 Butterworth pole location for n=2, and n=3 given by eqn. (2.33).

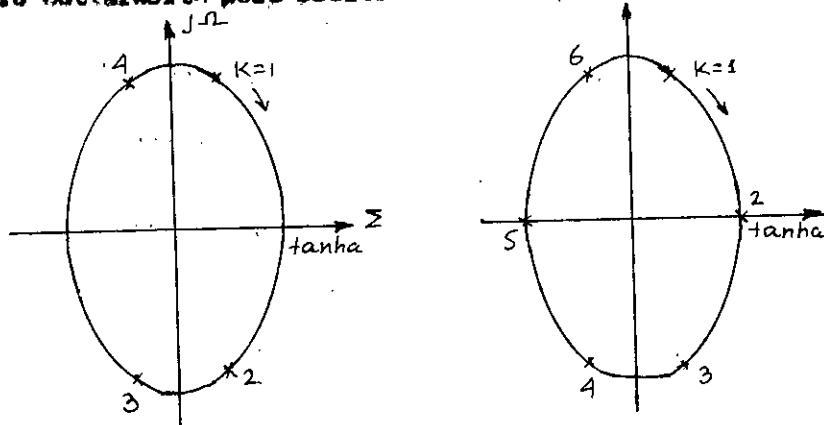


Fig.2.7. Chebyshev pole locations for n=2 end n=3.

Comprising the fig. 2.6 and Fig. 2.7 for the cases $n=2$ and $n=3$ we arrive at the following procedure to locate the poles for the Chebyshev case: Locate the poles on a unit circle using eqn. (2.33). Reduce the imaginary parts so obtained by multiplying by $\tanh \epsilon$ and this becomes the real part for the Chebyshev case. The real part from eqn. (2.33) is the imaginary part for the Chebyshev case directly.

But because of the different order of appearance for the two cases, fig. 2.6 and fig. 2.7, this procedure is simplified as : Locate poles for the Butterworth case using eqn. (2.4). Reduce the real part by multiplying $\tanh \epsilon$, but use the imaginary part directly. For example, for the Butterworth pole, $s = \sigma_1 + j\omega_1$, the corresponding Chebyshev pole is given by $s = \sigma_1 \tanh \epsilon + j\omega_1$, where $\epsilon = \frac{1}{n} \sinh^{-1} \frac{1}{\epsilon}$

2-3 Frequency Transformation from Low-pass to Bandpass:

Now we are in a position to determine the poles for lowpass filter. These poles must be transformed by a suitable frequency transformation in the appropriate band in order to have poles that gives the prescribed bandpass filter characteristic.

Let $p = \sigma + j\Omega$ represent the frequency for the lowpass function and $s = \sigma + j\omega$ represent the new frequency variable for the bandpass case. It is required to find a relation

$$p = x(\pi) \dots\dots(2.34)$$

between the variable p and s such that $x(s)$ must convert the frequency range $-1 \leq \Omega \leq 1$ of the lowpass characteristic to the desired frequency range $\omega_1 \leq \omega \leq \omega_2$ of the band pass response.

We now consider the lowpass to bandpass transformation. The lowpass attenuation characteristic which is to be transformed is shown in fig. 2.8. In this transformation we require that the pass band $-1 \leq \Omega \leq 1$ be divided into passbands, one on the positive axis and the other on the negative. Since the magnitude characteristic is an even function, we may consider the positive frequency range only.

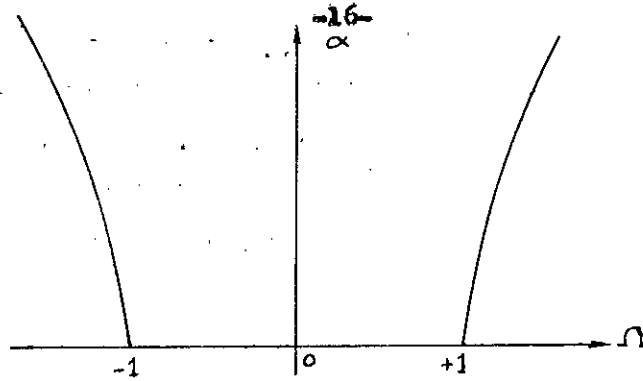


Fig. 2.8 : Lowpass attenuation characteristic.

Some of the particular points transformation needed are listed in table 2.1. These points are shown in fig. 2.9 which indicates the nature of the functional

Table 2.1

Points in $j\Omega$ - axis	Corresponding points in $j\omega$ - axis
$j\infty$	∞
$+j1$	$j\omega_2$
0	$j\omega_0$
$-j1$	$j\omega_1$
$-j\infty$	0

relation required between ω and Ω . This is strongly reminiscent the curve of the

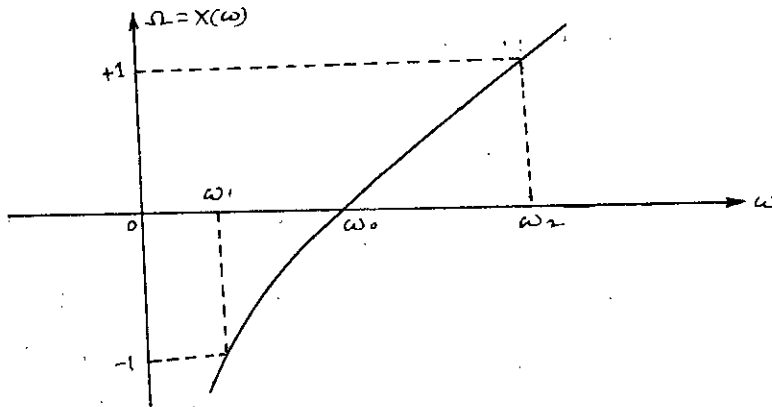


Fig. 2.9. Relation between ω and Ω

reactance of an inductor and capacitor in series which suggests the possible relation

$$\Omega = k_1 \omega = \frac{1}{k_2 \omega} \dots\dots\dots(2.35)$$

or, more generally

$$p = x(s) = k_1 \left(\frac{s}{\omega_0} + \frac{\omega_0}{s} \right) \dots\dots\dots(2.36)$$

Substituting $p = \pm j1$ and $s = j\omega$ in eqn. (2.36) we have

$$\omega^2 + \frac{\omega_0}{k_1} \omega - \omega_0^2 = 0 \dots\dots\dots(2.37)$$

The solutions of this equation are

$$\omega_1, \omega_2, \omega_3, \omega_4 = \omega_0 \pm \left[\frac{1}{2k_1} \pm \sqrt{\left(\frac{1}{2k_1}\right)^2 + 1} \right] \dots\dots\dots(2.38)$$

from this result, we have

$$\omega_1 \omega_2 = \omega_3 \omega_4 = \omega_0^2$$

$$\text{and } \omega_2 - \omega_1 = \omega_4 - \omega_3 = \frac{\omega_0}{k_1} = B$$

where B is the bandwidth of the transformed passband.

Eqn. (2.36) now becomes

$$p = \frac{\omega_0}{B} \left(\frac{s}{\omega_0} + \frac{\omega_0}{s} \right) \dots\dots\dots(2.39)$$

Where ω_0 is the geometric mean of the band-edge frequency and B is the bandwidth of the passband.

from equation (2.39)

$$s = \frac{\omega_0}{k} \left(kp \pm \sqrt{k^2 p^2 - 1} \right) \dots\dots\dots(2.40)$$

$$\text{Where } k = \frac{B}{2\omega_0} = \frac{\omega_2 - \omega_1}{2\omega_0} \dots\dots\dots(2.41)$$

If the lowpass pole positions are given in p - plane we can determine their bandpass positions in the actual complex plane s by using eqns.(2.40) and (2.41).

2.4 Example of frequency transformations:

With $n=3$, Lowpass Butterworth poles given by eqn.(2.4) are:

$$p_1 = -1.0 + j0.0$$

$$p_2 = -0.5 + j0.86603 \quad - (2.42)$$

$$p_3 = -0.5 - j0.86603$$

The corresponding lowpass Chebychev poles with $\frac{1}{2}$ db ripples ($\epsilon = 0.3493, \epsilon^2 = 0.1220$) are :

$$p_1 = -0.53089 + j0.0$$

$$p_2 = -0.26545 + j0.86603 \quad \dots\dots\dots(2.43)$$

$$p_3 = -0.26545 - j0.86603$$

The poles of eqns.(2.42) and (2.43) are shown in fig. 2.10.

These poles are transformed by using eqns. (2.40) and (2.41) in the passband

where $B = f_2 - f_1 = 40$ KHz

$$f_2 = \frac{w_2}{2\pi} = 475 \text{ KHz.}$$

$$f_1 = \frac{w_1}{2\pi} = 435 \text{ KHz.}$$

$$f_0 = \frac{w_0}{2\pi} = \sqrt{f_2 f_1}$$

and results, when normalized with respect to $2\pi \times 10^6$ are shown below

$$s_1 = -0.00511 + j0.43754$$

$$s_2 = -0.01062 + j0.45444 \quad \dots\dots\dots(2.44)$$

$$s_3 = -0.00551 + j0.47218.$$

The pole locations of eqn. (2.44) are shown in fig. 2.11.

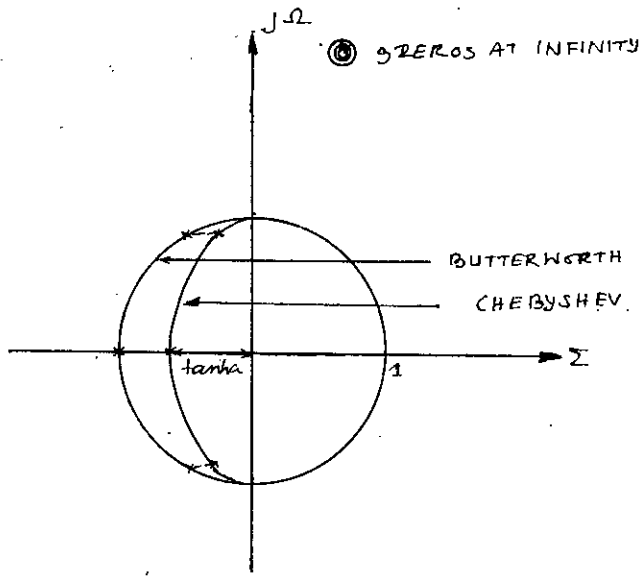


Fig. 2.10 Lowpass Butterworth and Chebyshev pole and zero locations.

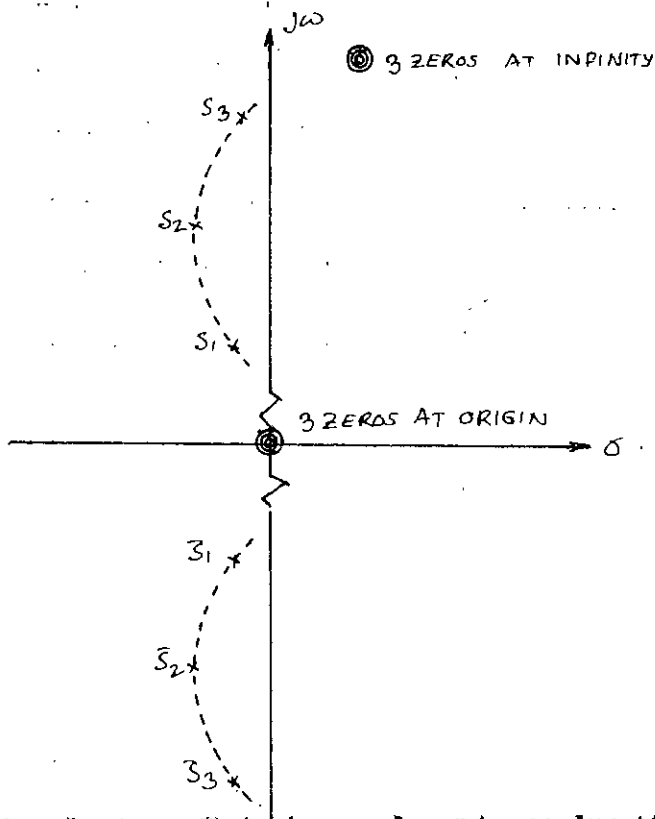


Fig.2.11 : Bandpass Chebyshev pole and zero locations.

CHAPTER -3

A GENERAL FILTER CIRCUIT

3.1 General Considerations

The use of electric wave filters in electronic equipment has increased as equipment has become more complex. Many subsystem operations rely on filters.

Electric wave filter can be classified by several different methods. In terms of the frequency spectrum they may be grouped as audio-frequency, radio-frequency, and microwave filters. In terms of the circuit configuration of the basic elements, filters may take the configuration of a ladder (in the form of T, L or Π) or a lattice. Classification in terms of the character of the elements is also common: LC filters, R-C filters etc. If a network has an internal source of energy, it may be termed as active filter. An IF amplifier is an example of an active network. Filters with no source of energy within the network are termed passive.

According to the nature of their frequency response, the filters can be classified as low-pass, highpass and bandpass. As this study is concerned with band-pass active filters, a few of the basic configurations of passive bandpass networks are discussed below.

Band-pass³¹: A band-pass filter (fig. 3-1) allows a band of frequencies from certain lower to upper limits to pass without or with negligible attenuation and stops all energy outside these two limits. This filter is by far the most important and most commonly used in electronic equipment.

A series-resonant circuit has maximum current and minimum impedance at the resonant frequency. Connected in series with R_L , as in fig. 3-1(a), the series-tuned LC circuit allows frequencies at and near resonance to produce maximum output across R_L providing a bandpass filter.

The parallel LC circuit connected across R_L , as shown in fig. 3.1(b), also provides a bandpass filter. At resonance the high impedance of the parallel LC circuit

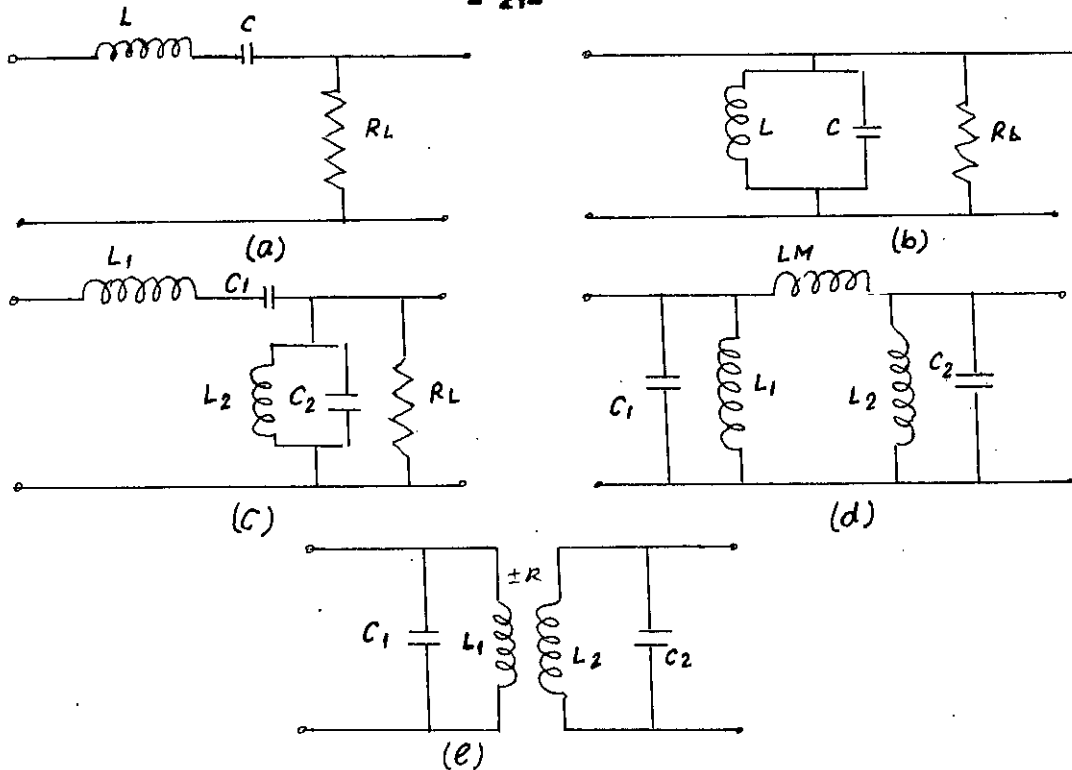


Fig. 3.1 Band-pass filter circuit. (a) series resonant, (b) parallel resonant, (c) Inverted L- type, (d) Ladder-type (e) double tuned type.

allows R_L to develop its output signal. Below resonance, R_L is shorted by the low reactance of L ; above resonance R_L is shorted by the low reactance of C . For frequencies at and near resonance, though, R_L is shunted by a high impedance, resulting in maximum output signal.

Series-and parallel- resonant circuits can be combined in L, T, or Π sections to improve the filtering as shown in fig. 3.1(C), (d) and (e).

In this chapter we will analyse a general cascaded transistorized filter circuit for band-pass characteristics and the nature and the configuration of the interstages that are placed between each pair of transistors.

3.2 - General analysis of an active filter circuit:

The general active filter circuit under consideration is shown in fig.3.2. It consists of n transistors and n passive interstages H_1, H_2, \dots, H_n .

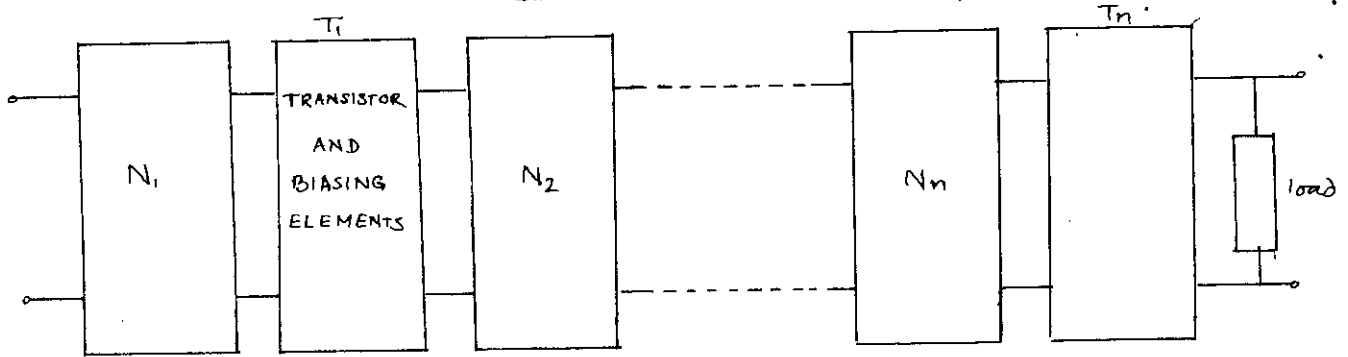


Fig. 3.2 A general filter circuit.

Replacing the transistors with their incremental high frequency hybrid-II models and using Miller effect¹² to simplify them, the filter circuit of fig. 3.2 is redrawn in fig. 3.3. It is observed that the complete network is now

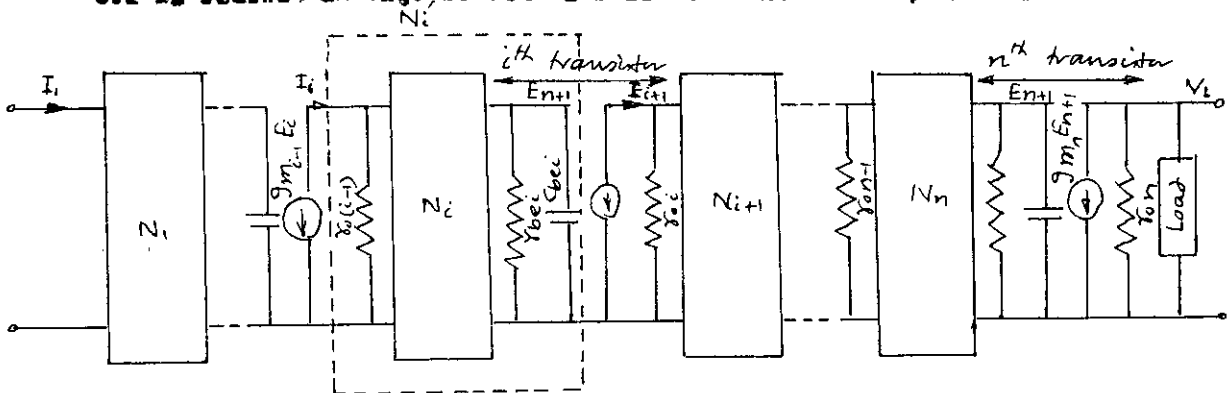


Fig.3.3: Incremental equivalent circuit of Fig. 3.2.

divided into n separate parts N'_i ($i = 1, 2, \dots, n$).

N'_i consists of interstage N_i , output resistance of $(i-1)^{th}$ transistor and the input resistance and capacitance of the i^{th} transistor. E_{i+1} is the output voltage of N'_i and controls the input current I_{i+1} of the N_{i+1} .

From fig. 3.3 the voltage across the load R'_L can be written as

$$V_L = (g_{m_n} E_{n+1}) R'_L \quad \dots \dots \dots (3.1)$$

where E_{n+1} is the voltage across the input of n^{th} transistor and R'_L is the parallel combination of r_{on} and the load R_L which is considered to be resistive.

The transfer function $\frac{V_L}{I_1}$ of the filter circuit thus becomes

$$\frac{V_L}{I_1} = \frac{g_n E_{n+1} R_L'}{I_1} \dots\dots\dots(3.2).$$

Now $\prod_{i=1}^n \frac{E_{i+1}}{I_i} = \frac{E_2}{I_1} \frac{E_3}{I_2} \dots\dots\dots \frac{E_{n+1}}{I_n} \dots\dots\dots(3.3)$

From fig. 3.3, the input voltage E_{i+1} and the output current I_{i+1} of the i th transistor are related by

$$I_{i+1} = g_{m_i} E_{i+1}, \quad i = 1, 2, \dots\dots\dots n \dots(3.4).$$

Designate the input current of the passive network N_i , I_i and its output voltage E_{i+1} . Let the transfer impedance $\frac{E_{i+1}}{I_i}$ of N_i be

$$\frac{E_{i+1}}{I_i} = f_i(s) \dots\dots\dots(3.5).$$

Substituting (3.4) and (3.5) in (3.3), we have

$$f_1(s) f_2(s) \dots\dots\dots f_n(s) = \frac{E_{n+1}}{I_1} \frac{1}{\prod_{i=1}^n g_{m_i}}$$

or $\frac{E_{n+1}}{I_1} = \prod_{i=1}^{n-1} g_{m_i} f_1(s) f_2(s) \dots\dots\dots f_n(s) \dots\dots\dots(3.6).$

Putting (3.6) in (3.2), we have the over-all transfer function as

$$Z_{12}(s) = \frac{V_2(s)}{I_1(s)} = \prod_{i=1}^n g_{m_i} R_L' f_1(s) f_2(s) \dots\dots\dots f_n(s) \dots\dots(3.7).$$

Where $f_i(s)$, $i = 1, 2, \dots\dots\dots n$, is the transfer function of N_i . From eqn.(3.7)

it is observed that the poles and zeros of $Z_{12}(s)$ are directly given by the critical frequencies of the transfer function $f_i(s)$. Therefore, the magnitude of $Z_{12}(j\omega)$ can be controlled by properly selecting the poles and zeros of $f_i(s)$.

3.3 Synthesis of the typical i th interstage.

A Typical i th interstage of the filter circuit is shown in fig. 3.4. It is evident from fig. 3.4 that N_i is to be synthesized in such a way that the interstage N_i must realize a certain number of poles and zeros of the over-all transfer

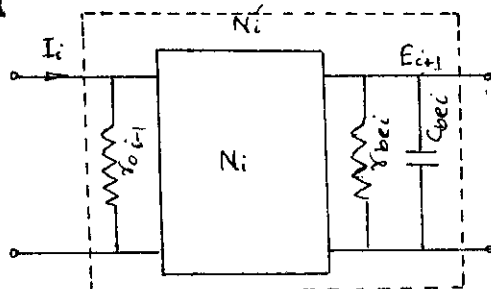


Fig. 3.4 : Typical i th interstage.

function or their modified locations that achieve the prescribed response.

Once the filter specifications are furnished, one can find rational function approximation to it following a standard procedure.

The way the poles and zeros of the transfer function of the filter are divided amongst the interstages N_i will determine their number and configuration. If, however the configuration of the interstage N_i is pre-selected, so that the nature of location and the number of the poles and zeros of its transfer function are fixed, the critical frequencies of the over-all transfer function must be compatible with these in addition to satisfying the design specification.

In this section, both these methods will be discussed.

3.4 : Realization of prescribed response with selected rational functions.

The procedure for finding the poles and zeros of transfer function that meets the given specification has been outlined in chapter 2. Once these poles and zeros determined, the networks N_i of Fig. 3.3 has to be synthesized to realize these. In this section, a synthesis procedure is given for this purpose.

The locations of the zeros and poles for a third order Chebyshev band-pass response is shown in fig. 3.5. All or a part of these poles and zeros must

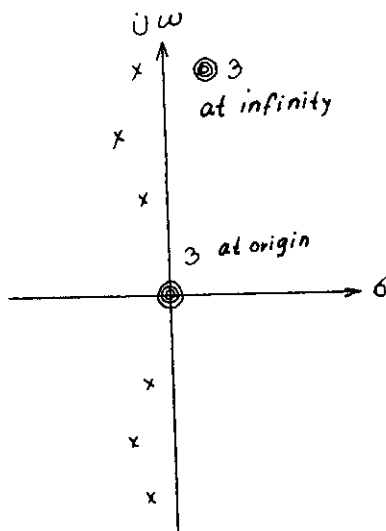


Fig.3.5, Pole and zero locations for a 3rd order Chebyshev bandpass response.

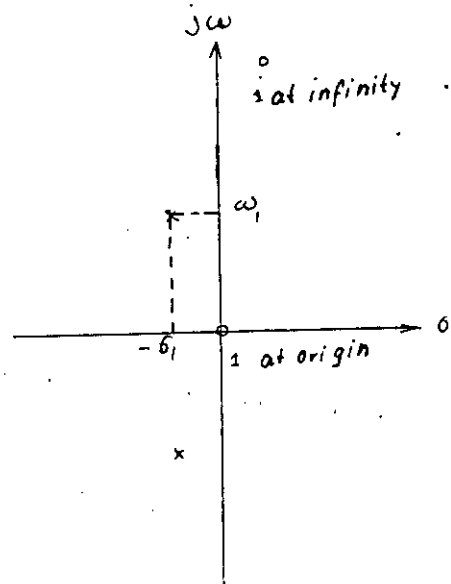


Fig.3.6 : Locations of pole and zero to be realized by each interstage.

be realized by interstage N_1' . In its simplest form, N_1' must at least realize a pair of poles and two zeros as shown in fig. 3.6.

The transfer function comprising the zeros and poles of Fig. 3.6 may be written as

$$T_1(s) = \frac{s}{s^2 + a_1 s + a_0} \dots \dots \dots (3.8)$$

Where $a_0 = \sigma_1^2 + \omega_1^2$, $a_1 = 2\sigma_1$.

This transfer function is to be synthesized to find the interstage network N_1' . The synthesis procedure is given below:-

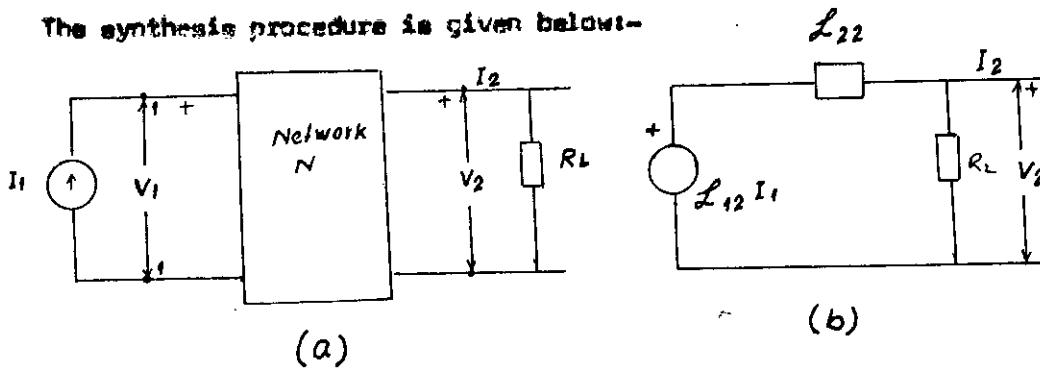


Fig. 3.7

Fig. 3.7(a) shows a network driven by a current source and terminated in a load resistance R_L . For this network, we will compute Z_{12} in terms of the open-circuit impedance functions z_{11} , z_{12} and z_{22} of lossless network N , making use of

Thevenin's Theorem. If the load is removed, the open-circuit output voltage is, from the definition of

$$z_{12} = \frac{V_2}{I_1} \Big|_{I_2=0}$$

$$V_{2OC} = z_{12} I_1 \quad \dots\dots\dots(3.9).$$

The Thevenin's equivalent impedance at terminals 2-2' is found by replacing the current source by an open circuit. This input impedance is z_{22} by definition, and the Thevenin's equivalent network is that shown in fig. 3.7(b). From this network,

$$\frac{V_2}{I_1} = z_{12} = \frac{z_{12} R_L}{z_{22} + R_L} \quad \dots\dots\dots(3.10).$$

If z_{12} is given, z_{12} and z_{22} can be found from eqn.(3.10). z_{12} and z_{22} can be synthesized by any standard procedure to obtain the network N.

With R_L normalized to 1Ω , from eqn. (3.8) and eqn. 3.10, we have

$$\frac{s}{s^2 + a_1 s + a_0} = \frac{z_{12}}{1 + z_{22}} \quad \text{from which } z_{12} \text{ and } z_{22} \text{ can be found as}$$

$$z_{12} = \frac{s}{s^2 + a_0}$$

$$\text{and } z_{22} = \frac{a_1 s}{s^2 + a_0}$$

It is evident that the realization of z_{12} and z_{22} is shown in fig. 3.8, where the load is also +

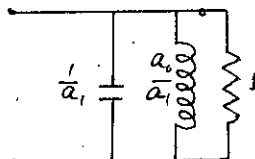


Fig. 3.8: i th interstage.

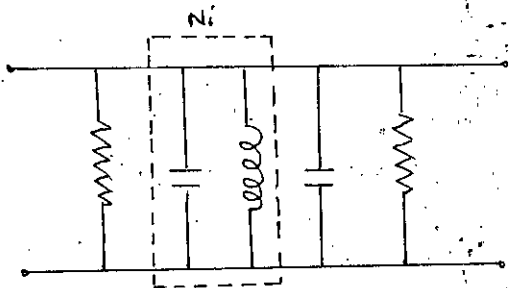


Fig.3.9: i-th interstage (modified form)

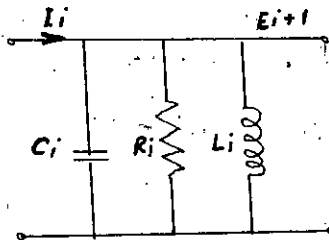


Fig.3.10: General form of the i-th interstage.

The resistance and the capacitance can be divided as shown in fig. 2.9. Now circuit of fig. 3.9 resembles that of the interstage N'_i as shown in fig.3.4 where N'_i is replaced by a capacitor and an inductor in parallel. When all the capacitors are combined together as well as the resistors, the general form of the interstage N'_i is shown in fig. 3.10.

The transfer function of fig. 3.10 is given by

$$Z_{12}(s) = \frac{E_{i+1}(s)}{I_i(s)} = \frac{K_i s}{s^2 + \frac{1}{R_i C_i} s + \frac{1}{L_i C_i}} \dots \dots \dots (3.11)$$

If the pole locations of fig. 3.6 is given by

$$s_1 = -\sigma_c + j\omega_1$$

$$-s_1 = -\sigma_c - j\omega_1$$

then the transfer function of eqn. (3.8) can be written as

$$f_i(s) = \frac{s}{(s - s_1)(s - \bar{s}_1)}$$

Putting the values of the poles and after simplification $f_i(s)$ becomes

$$f_i(s) = \frac{s}{s^2 - 2\sigma_c s + \sigma_c^2 + \omega_1^2} \dots \dots \dots (3.12)$$

Comparing eqn. (3.11) and eqn. (3.12), we have

$$\frac{1}{R_i C_i} = -2\sigma_c$$

and $\frac{1}{L_i C_i} = \sigma_i^2 + \omega_i^2 \dots\dots(3.13)$

Therefore, the interstage network (N_i') of fig. 3.10 can be used to realize the poles and zeros of fig. 3.6 and the elements are given the solutions of eqn.(3.13).

The interstage N_i' can also be used to realize two pair of poles and four zeros of the overall transfer function $Z_{12}(s)$, as shown in fig. 3.11.

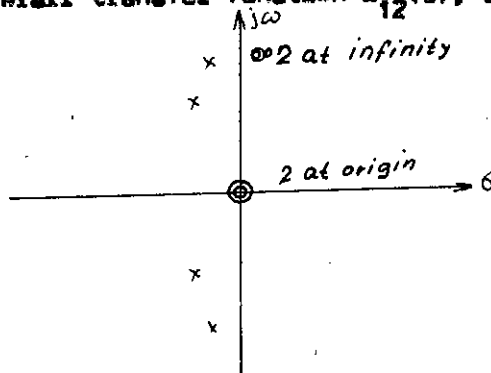


Fig.3.11: Locations of pole and zero to be realized by an interstage.

The transfer function comprising the poles and zeros of fig. 3.11 may be written as
$$f_i(s) = \frac{\Omega s^2}{s^4 + a_3 s^3 + a_2 s^2 + a_1 s + a_0} \dots\dots(3.14)$$

Where Ω is a constant.

This transfer function may be considered as transfer impedance $\bar{Z}_{12}(s)$ of a double terminated network of fig. 3.12.

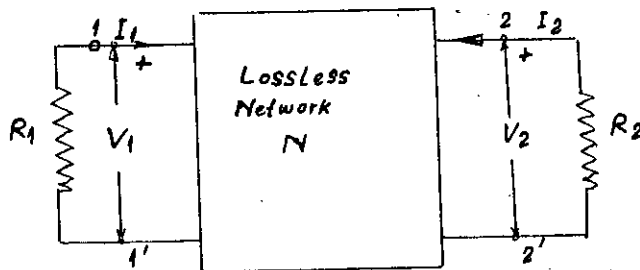


Fig. 3-12: Double terminated lossless network.

Therefore,
$$\bar{Z}_{12}(s) = \frac{\Omega s^2}{s^4 + a_3 s^3 + a_2 s^2 + a_1 s + a_0} \dots\dots(3.15)$$

The transmission coefficient $t(s)$ of fig. 3-12 is related to the transfer impedance $\bar{Z}_{12}(s)$ by the relation¹³

$$[t(s) t(-s)] = \frac{4 R_1}{R_2} [Z_{12}(s) \bar{Z}_{12}(-s)] \quad \text{-----(3.16)}$$

With $R_1 = R_2 = 1 \Omega$ and scale factor removed eqn.(3.16) becomes

$$[t(s) t(-s)] = [\bar{Z}_{12}(s) \bar{Z}_{12}(-s)] \quad \text{-----(3.17)}$$

The relationship between the transmission coefficient, $t(s)$ and the reflection coefficient ^{$\rho(s)$} is given

$$\rho(s)\rho(-s) = 1 - t(s) t(-s) \quad \text{.....(3.18)}$$

From eqn. (3.15), (3.17) and (3.18), we have

$$\rho = 1 - \frac{D s^2}{s^4 + a_3 s^3 + a_2 s^2 + a_1 s + a_0} - \frac{D s^2}{s^4 - a_3 s^3 + a_2 s^2 - a_1 s + a_0}$$

$$= \frac{b_6 s^6 + b_4 s^4 + (b_2 - D^2) s^2 + (b_0 - a_1^2)}{s^8 + b_6 s^6 + b_4 s^4 + b_2 s^2 + b_0} \quad \text{.....(3.19)}$$

where b_6, b_4, b_2 and b_0 can be written in terms of a_3, a_2, a_1 and a_0

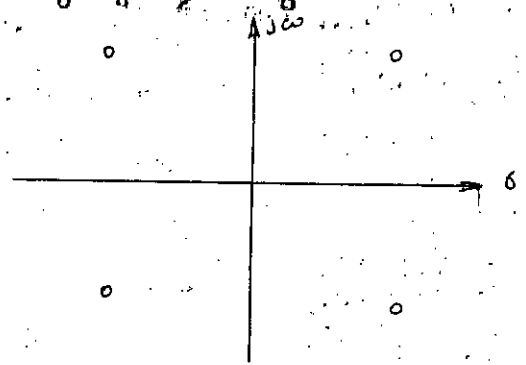


Fig. 3.13 ZEROS poles in quadrant symmetry.

The denominator of $\rho(s)$ is formed by multiplying those poles of the expression (3.19) which lie in the left half plane. The zeros of the numerator of the expression (3.19) are in quadrant symmetry, as shown in fig. 3.13. Since the

numerator of $p(s)$ need not be a Hurwitz polynomial, it is formed by the inclusion of a zero and its conjugate and rejecting the negative of these zeros.

Thus $p(s)$ can be written as

$$p(s) = \frac{c_4 s^4 + c_3 s^3 + c_2 s^2 + c_1 s + c_0}{s^4 + a_3 s^3 + a_2 s^2 + a_1 s + a_0} \quad (3-20)$$

The open circuit input impedance $Z_{11}(s) = \frac{V_2}{I_1} \Big|_{I_2=0}$ of fig. 3.12 can be formed from the relation $Z_{11}(s) = \frac{1-p(s)}{1+p(s)}$ (3.21)

Putting (3.20) into (3.21), we have

$$Z_{11}(s) = \frac{(1-c_4) s^4 + (a_3 - c_3) s^3 + (a_2 - c_2) s^2 + (a_1 - c_1) s + (a_0 - c_0)}{(1+c_4) s^4 + (a_3 + c_3) s^3 + (a_2 + c_2) s^2 + (a_1 + c_1) s + (a_0 + c_0)} \quad (3.22)$$

As all the transmission zeros lie at the origin and at the infinity, the function of eqn. (3.22), can be developed into a ladder form,

The cascade of several of such interstages give rise to an over-all transfer function that will have even number of poles. An extra single tuned circuit can be used to make the over-all transfer function have an odd number of poles if the situation warrants so.

3.5 : Realization of prescribed response with selected configuration of N_1^i

In this section we analyse the double terminated network of fig. 3.14 as a possible configuration for the interstage network N_1^i .

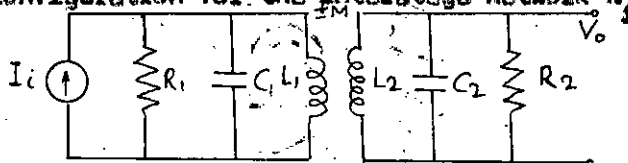


Fig.3.14 : Prescribed configuration of i th interstage.

The circuit of fig. 3-14 can be simplified by applying Thevenin's Theorem to the left of the points A-A' as shown in fig. 3.15.

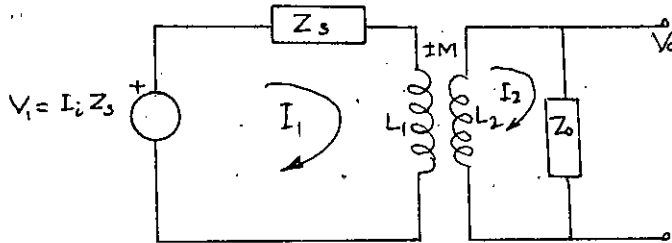


Fig. 3.15: Equivalent form of fig.3.14.

where $Z_s = \frac{R_1}{C_1 s}$

$$R_1 + \frac{1}{C_1 s}$$

$$Z_o = \frac{R_2}{C_2 s} = \frac{R_2 + \frac{1}{C_2 s}}$$

Let $Z_1 = Z_s + Z_1$

$Z_2 = Z_o + Z_2$

$Z_M = R_M \quad M = k \sqrt{L_1 L_2}$ where k is coefficient of coupling.

The loop equations from Fig. 3.15 are

$$Z_1 I_1 \pm Z_M I_2 = I_1 E_s \quad \text{---(3.23)}$$

$$\pm Z_M I_1 + Z_2 I_2 = 0 \quad \text{---(3.24)}$$

From eqns. (3-23) and (3-24), we have

$$I_2 = \frac{\begin{vmatrix} Z_1 & I_1 & Z_s \\ \pm Z_M & 0 & \end{vmatrix}}{\begin{vmatrix} Z_1 & \pm Z_M \\ \pm Z_M & Z_2 \end{vmatrix}} = \frac{-I_1 Z_s Z_M}{Z_1 Z_2 - Z_M^2} \quad \text{---(3.25)}$$

The output voltage V_o is

$$V_o = I_2 Z_o = \frac{-I_1 Z_H \beta}{Z_1 Z_2 - Z_M^2} Z_o \dots\dots\dots(3.26).$$

The transfer impedance is thus :

$$Z_{12}(s) = \frac{V_o}{I_1} = \frac{-Z_H \beta Z_o}{Z_1 Z_2 - Z_M^2} \dots\dots\dots(3.27).$$

Now $Z_1 = \frac{1}{R_1 + \frac{1}{C_1 s}} \left[\frac{R_1}{C_1 s} + s L_1 \left(R_1 + \frac{1}{C_1 s} \right) \right]$

$$= \frac{L_1 R_1}{s \left(R_1 + \frac{1}{C_1 s} \right)} \left[s^2 + \frac{1}{C_1 R_1} s + \frac{1}{L_1 C_1} \right]$$

Similarly $Z_2 = \frac{L_2 R_2}{s \left(R_2 + \frac{1}{C_2 s} \right)} \left[s^2 + \frac{1}{C_2 R_2} s + \frac{1}{L_2 C_2} \right]$

Putting values of Z_1 , Z_2 , Z_o , Z_M and Z_H into (3.27), we have

$$Z_{12}(s) = \frac{k}{L_1 L_2 C_1 C_2 (1-k^2)} \frac{s}{s^4 + a_3 s^3 + a_2 s^2 + a_1 s + a_0} \dots\dots\dots(3.28)$$

where

$$a_3 = \frac{1}{C_2 R_2} + \frac{1}{L_1 R_1}$$

$$a_2 = \left[\left(\frac{1}{L_1 C_1} + \frac{1}{L_2 C_2} \right) / (1-k^2) \right] + \frac{1}{R_1 R_2 C_1 C_2}$$

$$a_1 = \left(\frac{1}{L_2 C_2 C_1 R_1} + \frac{1}{L_1 C_1 C_2 R_2} \right) / (1-k^2) \dots\dots\dots(3.29)$$

$$a_0 = \frac{1}{L_1 C_1 L_2 C_2 (1-k^2)}$$

The transfer function of eqn. (3.28) has (i) two pair of poles at finite frequencies and (ii) four zeros - one at the origin and other three at infinity.

The pole distribution is similar to that of Chebyshev or Butterworth bandpass response, but the zero distribution is different. In Butterworth or Chebyshev bandpass response the zeros are equally divided between the origin and the infinity of the s-plane, whereas for the case under consideration they are not. As the number of zeros at infinity is more than that at the origin, the frequency response of the network of fig. 3.14 with Chebyshev poles, will decrease sharply after the centre frequency as the input frequency go on increasing. Thus the circuit of fig. 3.14 provides with an unsymmetrical frequency response characteristics as shown in fig. 3.16. As the location of the zeros are fixed because of selected configuration of the interstage, the pole locations must be adjusted to be compatible with frequency response characteristic as demanded by the design specification.

The denominator of eqn. (3.20) cannot be factored in general. Such networks must be synthesized either by approximation or coefficient matching. In coefficient matching, a desired polynomial is set up and the coefficients a_0, a_1, a_2 and a_3 are equated to the numerical values of the coefficients of the known polynomial. This method can always be employed providing the network is capable of having poles and zeros in the desired positions.

Now if the pole locations of fig. 3.11 or their adjusted ones are given by

$$\begin{aligned}
 s_1 &= \sigma_1 + j\omega_1 \\
 \bar{s}_1 &= \sigma_1 - j\omega_1 \\
 s_2 &= \sigma_2 + j\omega_2 \\
 \bar{s}_2 &= \sigma_2 - j\omega_2
 \end{aligned}
 \tag{3.30}$$

A general transfer function comprising these poles and four zeros, one at the origin and other three at infinity, is constructed as

$$f_1(s) = \frac{0.5}{(s-s_1)(s-\bar{s}_1)(s-s_2)(s-\bar{s}_2)}$$

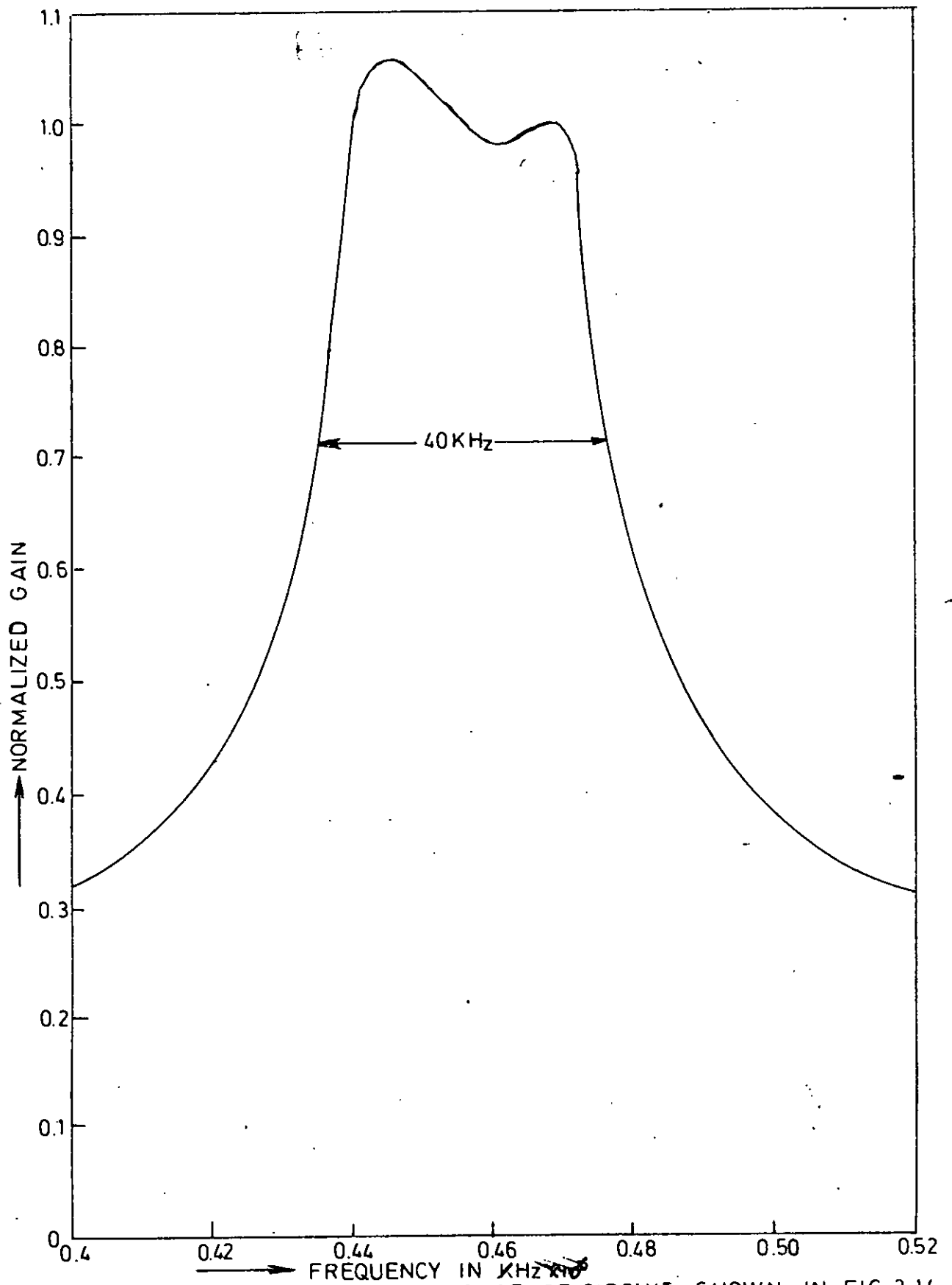


FIG 3.16 FREQUENCY RESPONSE OF CIRCUIT SHOWN IN FIG.3.14

Putting the values of the poles, $f_1(s)$ becomes

$$f_1(s) = \frac{D_1 S}{(s - \sigma_1 - j\omega_1)(s - \sigma_1 + j\omega_1)(s - \sigma_2 - j\omega_2)(s - \sigma_2 + j\omega_2)} \quad \text{---(3.31)}$$

Simplifying eqn. (3.31) and comparing with eqn. (3.20), we have

$$\frac{1}{C_1 R_1} + \frac{1}{C_2 R_2} = -2(\sigma_1 + \sigma_2)$$

$$\left[\left(\frac{1}{L_1 C_1} + \frac{1}{L_2 C_2} \right) / (1 - k^2) \right] + \frac{1}{R_1 R_2 C_1 C_2} = \sigma_1^2 + \omega_1^2 + 4\sigma_1 \sigma_2 + \sigma_2^2 + \omega_2^2$$

$$\left(\frac{1}{L_2 C_2 C_1 R_1} + \frac{1}{L_1 C_1 C_2 R_2} \right) / (1 - k^2) = -2\sigma_2(\sigma_1 + \omega_1^2) + 2\sigma_1(\sigma_2^2 + \omega_2^2)$$

$$\frac{1}{L_2 C_2 L_1 C_1 (1 - k^2)} = (\sigma_1^2 + \omega_1^2)(\sigma_2^2 + \omega_2^2) \quad \dots(3.32)$$

Solution of the set of equations (3.32) gives the values of $R_1, R_2, L_1, L_2, C_1, C_2$ and K of the network in Fig. 3.14.

3.5.1 Method for solution of Eqn. (3.32) :

With loose coupling i.e. $K \ll 1$ and with $\sigma_1 \ll \omega_1$ and $\sigma_2 \ll \omega_2$ which are the usual cases, the eqn. (3.32) can be approximated as

$$\frac{1}{C_1 R_1} + \frac{1}{C_2 R_2} \approx -2(\sigma_1 + \sigma_2)$$

$$\frac{1}{L_1 C_1} + \frac{1}{L_2 C_2} + \frac{1}{R_1 R_2 C_1 C_2} \approx \omega_1^2 + \omega_2^2$$

$$\frac{1}{L_2 C_2 C_1 R_1} + \frac{1}{L_1 C_1 C_2 R_2} \approx -(2\sigma_2 \omega_1^2 + 2\sigma_1 \omega_2^2) \dots(3.33)$$

$$\frac{1}{L_2 C_2 L_1 C_1} \approx \omega_1^2 \omega_2^2$$

Let $\frac{1}{C_1 R_1} = x$, $\frac{1}{C_2 R_2} = y$, $\frac{1}{L_1 C_1} = z$ and $\frac{1}{L_2 C_2} = w$.

The eqn.(3.33) now can be written as

$$x + y = a \quad (3.34 a)$$

$$z + w + xy = b \quad (3.34b)$$

$$zy + wx = c \quad (3.34c)$$

$$zw = d \quad (3.34 d)$$

The right members

$$a = -2(\delta_1 + \delta_2)$$

$$b = w_1^2 + w_2^2$$

$$c = -(2\delta_2 w_1^2 + 2\delta_1 w_2^2)$$

$$d = w_1^2 w_2^2$$

are all positive so long as δ_1 and δ_2 remain negative i.e. the pole locations remain in the left half of the s-plane.

Let us consider two of the pole locations of a sixth order Chebyshev filter with $\frac{1}{4}$ db ripple, bandwidth of 40 KHz and centre frequency equal to 455 KHz that will be realized by the network of fig.3.14. These are

$$S_1 = (-0.00168 + j0.43565) 2\pi \times 10^6$$

$$S_2 = (-0.00465 + j0.44061) 2\pi \times 10^6$$

From these pole locations

$$\delta_1 = -0.00168 \times 2\pi \times 10^6$$

$$\delta_2 = -0.00465 \times 2\pi \times 10^6$$

$$w_1 = 0.43565 \times 2\pi \times 10^6$$

$$w_2 = 0.44061 \times 2\pi \times 10^6$$

The right hand side of eqn. (3.34a) is of the order of 10^4 . Thus both x and y , is of the order of 10^4 or less. In eqn. (3.34b) w_1^2 and w_2^2 is of the order of 10^{12} . Thus the product xy may be neglected compared with w_1^2 and w_2^2 .

Therefore the eqn. (3.34b) can be written as

$$z + w = b \quad \dots\dots\dots(3.35a)$$

from eqn. (3.34c),

$$\frac{z/c}{y} + \frac{y/c}{x} = 1 \quad \dots\dots\dots(3.35b)$$

where c/y and c/x are each of the order of w_1^2

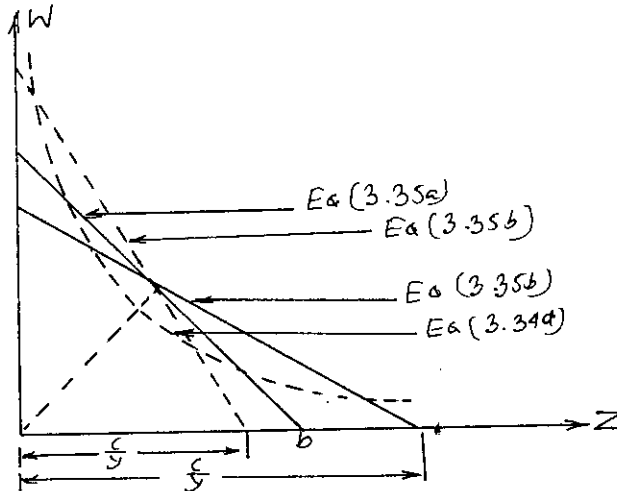


Fig.(3.17) : Graphical representation of eqn.(3.35a), (3.35b), (3.34d) .

The graphical representations of eqn. (3.35a), eqn. (3.35b) and eqn. (3.34d) are shown in fig. 3.17, which shows that solutions of eqns. (3.35a), eqn.(3.35b) and eqn. (3.34d) exists in the first quadrant. However, this solution affected by the choice of x and y . Eqn. (3.34a), $x + y = -2(\sigma_1 + \sigma_2) = a$, shows that infinite number of choices of x and y can be made. But since $x = \frac{1}{C_1 R_1} = \frac{w_1}{r_q}$ and $y = \frac{1}{C_2 R_2} = \frac{w_2}{q_2}$, too small a choice for the value of either x or y leads to large value of Q of corresponding coil. This may be unacceptable from the point of view of physical realizability. Selecting x and y to be nearly equal thus gives the best solution and ensures minimum possible Q 's for both coils. A computer program has been prepared to solve the equations(3.32) exactly. Thus with these pole locations, the simultaneous solution of the non-

linear eqn. (3.32) give positive values of the parameters which is a prerequisite condition for physical realizability.

Several interstages of fig. 3-14 each of which realizes a prescribed set of poles and zeros can be cascaded to give a single over-all maximally flat, equi-ripple, linear-phase, or similar function, having an even number of poles. An extra single-tuned circuit can be used to make the over-all function have an odd number of poles. Such systems have been called "stagger damped"¹⁵ because the most observable physical difference between the various interstages is the difference in the loading resistors.

CHAPTER-4

ACTIVE FILTER DESIGN WITH SINGLE TUNED INTERSTAGES:

In the last chapter , two methods of synthesizing transistor interstage for specified response have been given. This chapter provides an example of transistor amplifier design with three interstages when the response of the amplifier was prescribed, using the first method.

4-1 Specifications of amplifier response:

It is required to design a bandpass filter with ± 1 db tolerance in the pass-band, having centre frequency $f_0 = 455$ KHz, 3-db bandwidth 40 KHz. Also the magnitude of the transfer function must be at least 15 db/ $\frac{d^2\omega}{dt^2}$ at $f_x = 500$ KHz from its value at the centre frequency, f_0 .

Determination of transfer function for lowpass response:-

We will have to calculate n for the required magnitude characteristic which will determine the number of poles of the transfer function.

for bandpass characteristic:

Centre frequency, $f_0 = 455$ KHz

Band edges are $f_2 = 475$ KHz

$f_1 = 435$ KHz

Magnitude condition is given at $f_x = 500$ KHz.

The corresponding points in the lowpass magnitude characteristic can be obtained using the frequency transformation given by the relation of eqn.(2-39).

These points are

points in band pass	Corresponding points in low pass
j 455 KHz	0
j 475 KHz	$j 1$
j 435 KHz	$-j1$
j 500 KHz	$j2$

The lowpass Chebyshev characteristic is represented by the expression.

$$|Z_{12}|^2 = \frac{1}{1 + \epsilon^2 c_n^2(\Omega)}$$

For 1/2 db ripple, $\epsilon = 0.3493$, $\epsilon^2 = 0.1220$.

Since the magnitude characteristic remains unchanged by the frequency transformation, we can write as required by the specification.

$$\frac{1}{1 + \epsilon^2 c_n^2(2)} = 10^{-105}$$

$$\text{or, } 1 + \epsilon^2 c_n^2(2) = 22.4$$

$$\text{or, } c_n(2) = 13.25 \quad \text{---(A)}$$

Put $c_n(A) = 2^{(n-1)} \Omega^n$ retaining only the first term of the Chebyshev Polynomial.

With $n = 2$

$$c_2(2) = 8$$

with $n = 3$

$$c_3(2) = 32$$

Therefore $n=3$ meets the specification.

For $n = 3$, lowpass Butterworth poles (left half plane) are :

$$P_1^* = 1.0 + j0.0$$

$$P_2^* = -0.5 + j0.86603 \quad \dots\dots\dots(4.1)$$

$$P_3^* = -0.5 - j0.86603$$

and the corresponding lowpass Chebyshev poles with 1/2 db ripple are :

$$P_1 = -0.53009 + j0.0$$

$$P_2 = -0.26545 + j0.86603 \quad \dots\dots\dots(4.2)$$

$$P_3 = -0.26545 - j0.86603.$$

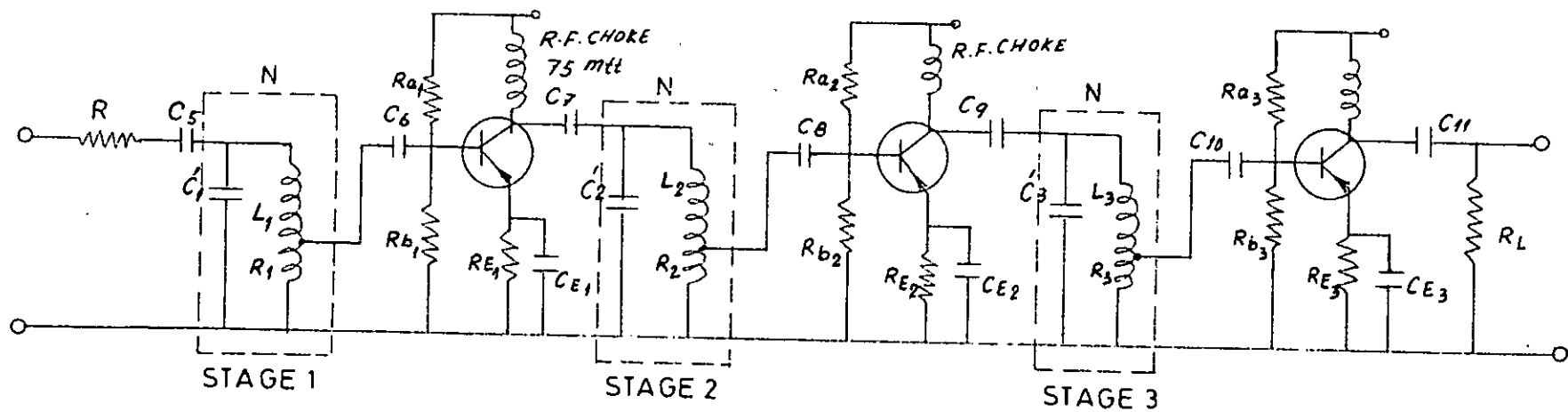


FIG. 4.1 ACTUAL FILTER CIRCUIT

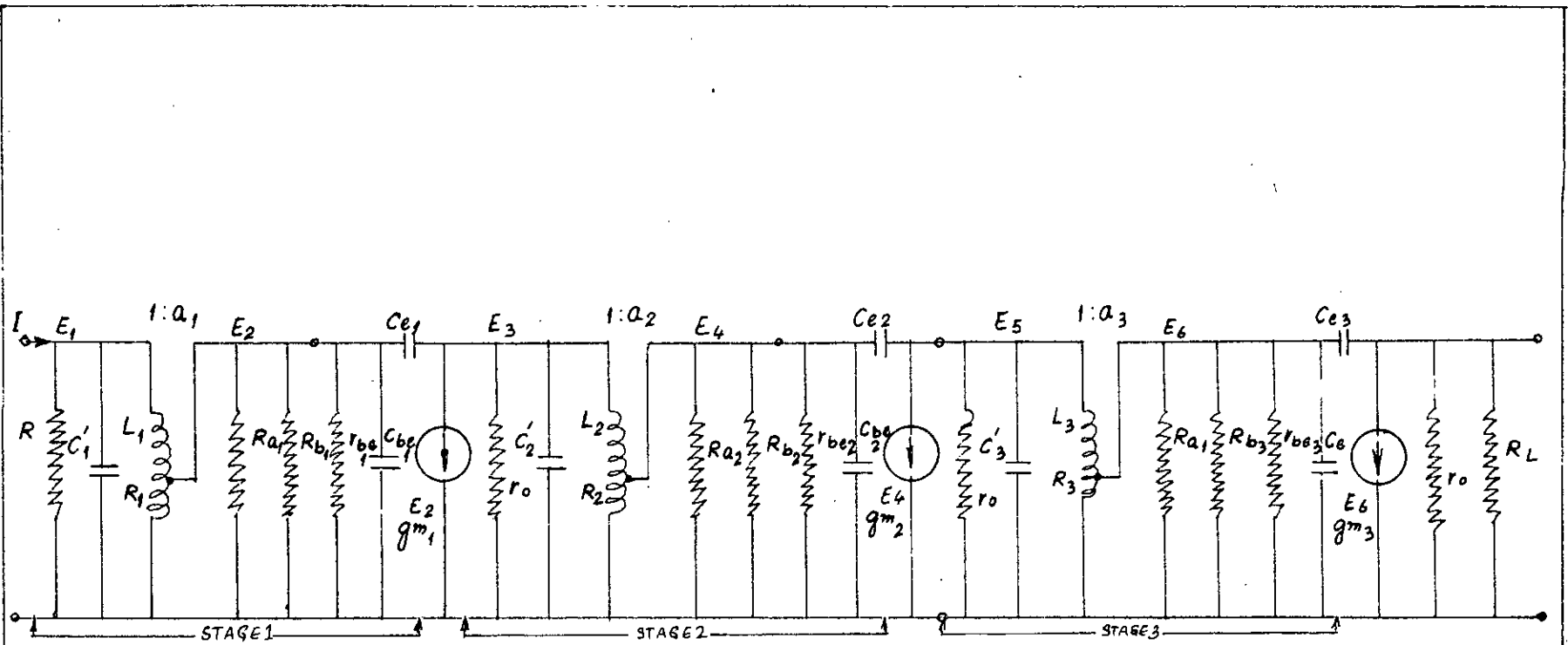


FIG. 4.2 EQUIVALENT CIRCUIT

The lowpass transfer function now becomes

$$Z_{12}(p) = \frac{1}{(p-p_1)(p-p_2)(p-p_3)} \dots\dots\dots(4.3).$$

4.2 Determination of bandpass poles and zeros:

The poles given in eqn. (4.2) are now transformed by lowpass to bandpass transformation, eqn. (2-40) and (2.41). Here

$$B = f_2 - f_1 = 40 \text{ KHz}$$

$$f_2 = 475 \text{ KHz}$$

$$f_1 = 435 \text{ KHz}$$

$$f_0 = \sqrt{f_1 f_2}$$

The programme used for frequency transformation is given in Appendix B. The required poles (normalized by 2×10^6) are given below:

$$s_1 = 0.00511 + j0.43754$$

$$s_2 = 0.01062 + j0.45444 \dots\dots\dots(4.4)$$

$$s_3 = 0.00531 + j0.47218$$

Therefore in bandpass case, the transfer function is

$$Z_{12}(s) = \frac{s^3}{(s-s_1)(s-\bar{s}_1)(s-s_2)(s-\bar{s}_2)(s-s_3)(s-\bar{s}_3)} \dots\dots\dots(4.5)$$

Of six zeros, three are at the origin and the other three at infinity. This transfer function meets the desired specification. The interstages H_i of fig. 3.2 have to be so designed that the amplifier realizes the transfer function (4.5).

4.3 Detailed considerations of a typical stage :

Assigning each interstage to achieve one pair of poles, the amplifier

consists of 3 interstages. Fig. 3.2 with transistors and biasing elements is shown in fig. 4.1. The tapings are used for impedance matching purpose. The equivalent circuit is shown in fig. 4.2.

Now consider a typical stage such as stage 3 of fig. 4.2 and is redrawn in fig. 4.3.

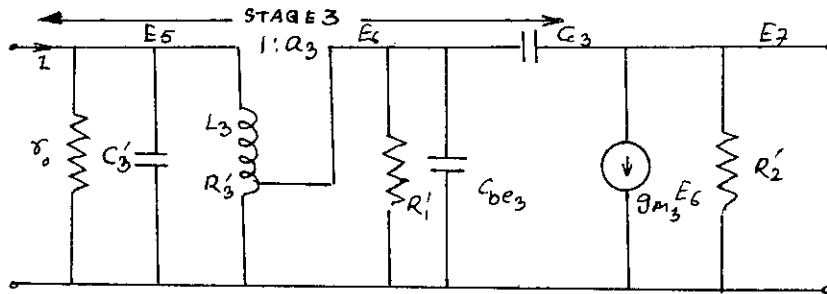


Fig.4.3 : A stage of the filter circuit of fig. 4.1.

Where

$$R_1' = R_{e3} \parallel R_{h3} \parallel r_{be3}$$

$$R_2' = \frac{r_o R_L}{r_o + R_L}$$

Using Miller effect the collector capacitance C_{c3} can be replaced by an equivalent capacitance connected between b' and ground as shown in fig.4.4, where $A_3 = g_{m3} \frac{r_o R_L}{r_o + R_L}$ (4.6).

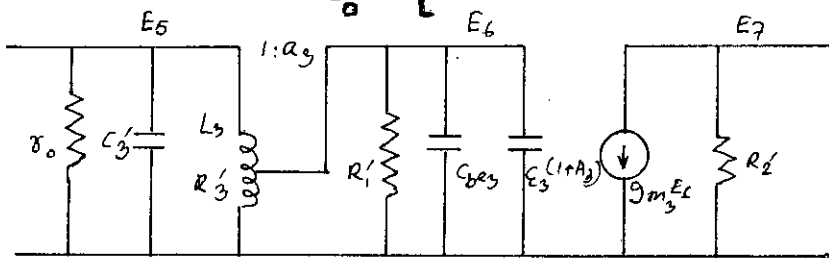


Fig.4.4. Net work of Fig. 4.3 after simplification.

The circuit of fig. 4.4 can further be simplified to the circuit in fig.4.5.

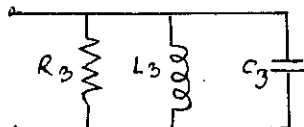


Fig.4.5 : Simplified form of the stage of fig. 4.3.

where $R_2 = r_o \parallel R_1' / a_3^2 \parallel / R_{p3}$ -----(4.7).

$R_{p3} = L_3 / C_3 R_3'$, parallel equivalent of the series resistance R_3' of the inductance L_3 .

$$C_3 = C_3' + a_3^2 C_{t3}$$

$$C_{t3} = C_{be3} + C_{c3} (1 + A_3)$$
 -----(4.8)

$$a_3 = E_6 / E_5$$

This simplified stage resembles the interstage network of fig. 3.10, this stage is to realize the poles $S_2 = -0.01062 \pm j0.45444$ for which

$$1 / R_3 C_3 = -2 \operatorname{Re} S_2 (2 \pi \times 10^6) = 0.02124 \times 2 \pi \times 10^6$$

and $1 / L_3 C_3 = S_2 (2 \pi \times 10^6)^2 = 0.20664 (2 \pi \times 10^6)^2$

If $L_3 = 0.0757$ mh, then

$$C_3 = 1625 \text{ pf}$$
 -----(4.9)

and $R_3 = 4.85 \text{ K}$ -----(4.10)

From eqn. (4.7)

$$R_3 = r_o \frac{1}{a_3} \parallel R_{a3} \parallel R_{b3}' \parallel r_{bc3} \parallel R_{p3}$$
 -----(4.11)

From eqn. (4.8)

$$C_3 = C_3' + a_3^2 [C_{be3} + C_{c3} (1 + A_3)]$$
 -----(4.12)

R_{a3} , R_{b3} , r_{bc3} and C_{be3} depend on the quiescent point. Therefore, the quiescent point and the value of a_3 must be selected in such a way that (i) R_3 given by eqn.(4.11) is not less than 4.85 K and (ii) the value of $a_3^2 [C_{be3} + C_{c3} (1 + A_3)]$ is not greater than 1625 pf. To meet both requirements, few trials, to determine the quiescent point, may be required.

For stages 2 and 1 exactly similar equations are obtained.

4.4 Design for a specified quiescent point

A typical D.C. stage of the filter circuit is shown below (fig.4.6)

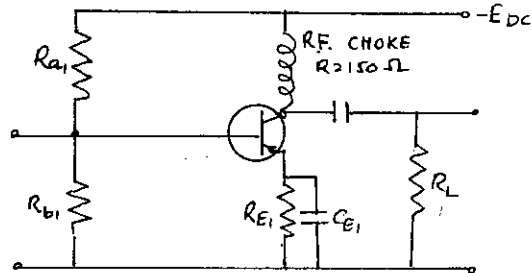


Fig. 4.6. A typical D.C. stage of the filter circuit of fig.4.1.

D.C. equivalent of fig. 4.6 is shown below.

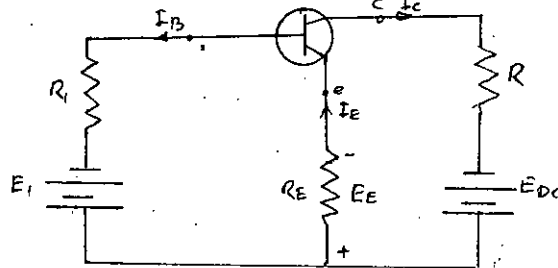


Fig. 4.7 D.C. equivalent of fig. 4.6. where base

Where base-biasing circuit is replaced by its Thevenin's equivalent, E_1 and R_1

$$E_1 = \left(\frac{R_{b1}}{R_{a1} + R_{b1}} \right) E_{DC} \text{ and } R_1 = \frac{R_{a1} R_{b1}}{R_{a1} + R_{b1}} \text{ -----(4.13)}$$

Now $E_{CE} = E_{DC} - R I_c - R_E I_E$

But $I_c = I_E$

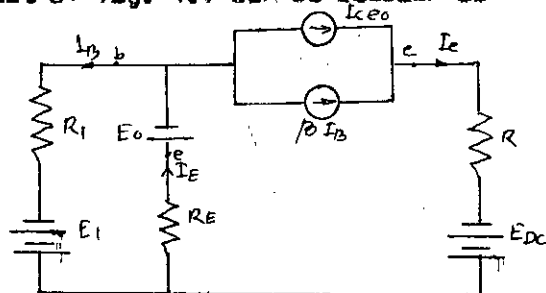
$$E_{CE} = E_{DC} - (R + R_E) I_c$$

$$I_c = E_{DC} / (R + R_E) - (E_{CE} / (R + R_E)) \text{ -----(4.14)}$$

$$I_c = I_D - E_{CE} / (R + R_E)$$

Where $I_D = E_{DC} / (R + R_E)$

The circuit of fig. 4.7 can be redrawn as



Now $E_1 - E_0 = R_1 I_B + R_E (I_B + I_C)$

and $I_C = I_B + I_{CEO}$

$E_1 - E_0 = [(R_1 + R_E) / \beta] (I_C - I_{CEO}) + R_E I_C$

Solving for I_C , we have

$$I_C = (R_E E_1 - E_0) / (R_1 + (1 + \beta) R_E) + [(R_1 + R_E) / (R_1 + (1 + \beta) R_E)] I_{CEO} \quad \text{---(4.5)}$$

The coefficient multiplying I_{CEO} in eqn.(4.15) is always less than unity and typically it is 0.1 or less. Thus I_{CEO} has a negligible effect on the quiescent point at room temperature and I_C can be calculated to a good approximation from

$$I_C = (E_1 - E_0) / (R_1 + (1 + \beta) R_E) \quad \text{---(4.16)}$$

Where $E_0 = 0.2$, in germanium transistor

= 0.6, in silicon transistor.

4.5 Determination of values of parameters for each Interstage:

Stage 3

To determine the quiescent current, D.C. parameters and transistor parameters, we consider the emitter current $I_E = 1 \text{ mA}$ and supply $E_{DC} = 6 \text{ V}$.

For 2N1683 transistor, $\beta = 80$ (Appendix A)

Base current = $I_C / \beta = I_E / \beta = 12.5 \mu\text{A}$

Let the bleed current be $125 \mu\text{A}$.

Current flowing through $R_{e3} = 125 + 12.5 = 137.5 \mu A$

Let the voltage across $R_{e3} = 1V$

$$R_{e3} = 1V / I_E = 1 K.$$

Therefore, voltage across $R_{b3} = 1 + 0.2 = 1.2V$

$$R_{b3} = 1.2V / 125 \mu A \approx 10 k.$$

Voltage across $R_{c3} = E_{DC} - 1.2 = 4.8 V.$

$$R_{c3} = 4.8 V / 137.5 \mu A \approx 33k$$

From eqn. (4.13),

$$R_1 = 7.68k$$

$$E_1 = 1.395v$$

From eqn. (4.16),

$$I_C = 1.08 mA.$$

for 2N1683 transistor,

$$f_T = 50 MHz, h_{fe} = 100, h_{re} = 3.36 \times 10^{-4}, C_C = 12pf$$

$$g_{m3} = qI_C / KT = 0.0432 mho$$

$$r_{be3} = h_{re} / g_{m3} = 1.89K$$

$$C_{be3} = g_{m3} / 2 f_T = 137.5pf$$

$$r_o = 1 / h_{re} g_{m3} = 69K$$

A.E. load is taken to be 4.7K.

To realize the poles $s_2 = (-0.01062 \pm j0.45444) 2\pi \times 10^6$ by this stage, we have

$$1/R_3 C_3 = -\text{Re}s_2 = 0.02124 \times 2\pi \times 10^6 \quad \text{-----(4.17)}$$

$$\text{and } 1/L_3 C_3 = |s_2|^2 = 0.20664 (2\pi \times 10^6)^2 \quad \text{-----(4.18)}$$

From eqn. (4.6)

$$A_3 = 190$$

For $L_3 = 0.0757 mH$, we have $R_{p3} = 30K$ at 454 KHz.

From eqn. (4.18)

$$C_3 = 1625pf$$

From eqn. (4.17)

$$R_3 = 4.05K$$

$$R'_1 = R_{a3} \parallel R_{b3} \parallel r_{e3}$$

$$R'_1 = 1.5 \text{ K}$$

From Eqn. (4.7)

$$R'_3 = r_o \parallel R_x \parallel R_{p3} \quad \text{where } R_x = R'_1 / a_3^2$$

$$R_x = 6.3 \text{ k.}$$

$$a_3^2 = R'_1 / R_x = .238$$

$$a_3 = 0.488$$

From eqn. (4.8)

$$C_{t3} = 2429.5 \text{ pf}$$

$$C'_3 = C_3 - a_3^2 C_{t3} = 1035 \text{ pf.}$$

Stage 2

For the same operating point as stage 3, the d.c. parameters and transistor parameters have the values as calculated for stage 3.

To realize the poles $S_1 = (-0.00511 + j0.43754) 2\pi \times 10^6$ by stage 2, we have

$$1/R_2 C_2 = 0.01027 \times 2\pi \times 10^6 \quad \text{-----4.19.}$$

$$\text{and } 1/L_2 C_2 = 0.19173 (2\pi \times 10^6)^2 \quad \text{-----4.20.}$$

From eqn. (4.6),

$$A_2 = g_{m2} R_3 = 210$$

For $L_2 = 0.0839 \text{ mh}$, $R_{p2} = 30\text{k}$ at 437 KHz.

From eqn. (4.20)

$$C_2 = 1580 \text{ pf.}$$

from eqn. 4.19

$$R_2 = 9.95 \text{ K.}$$

$$R'_1 = R_a = 1.5 \text{ K.}$$

From Eqn. 4.7

$$R_2 = r_o \parallel R_x \parallel R_{p2} \text{ where } R_x = R_{x1} / a_2^2$$

$$\text{or } R_x = 18.1 \text{ K.}$$

$$a_2 = 0.288$$

From eqn. 4.8.

$$C_{t2} = 2669.5 \text{ pf.}$$

$$C_2' = C_2 - a_2^2 C_{t2} = 1356 \text{ pf.}$$

Stage 1

The operating point of stage 1 is same as the other two stages and it realizes the poles $S_3 = (-0.00581 + j0.47218) 2\pi \times 10^6$, so that we have

$$1/R_1 C_1 = 0.01102 \times 2\pi \times 10^6$$

-----4.21

$$\text{and } 1/L_1 C_1 = 0.22325 (2\pi \times 10^6)^2$$

-----4.22

From eqn. 4.6

$$A_1 = g_{m1} R_2 = 421.$$

For $L_1 = 0.0717 \text{ mh}$, $R_{p1} = 25 \text{ k}$ at 472 KHz.

From eqn. 4.22 $C_1 = 1586 \text{ pf.}$

From eqn. (4.21)

$$R_1 = 9.15 \text{ K.}$$

$$R_{x1} = 2.5 \text{ k.}$$

From eqn. (4.7) $R_1 = R_p \parallel R_x \parallel R_{p1}$ where $R_x = R_{x1} / a_1^2$

$$R_x = 16 \text{ k.}$$

$$a_1 = 0.306$$

$$C_{t1} = C_{Del} + C_{c1} (1 + A_1) = 5201.5 \text{ pf.}$$

$$C_1' = C_1 - a_1^2 C_{t1} = 1100 \text{ pf.}$$

Calculated parameter values are shown in the attached circuit (Fig 4.1A)

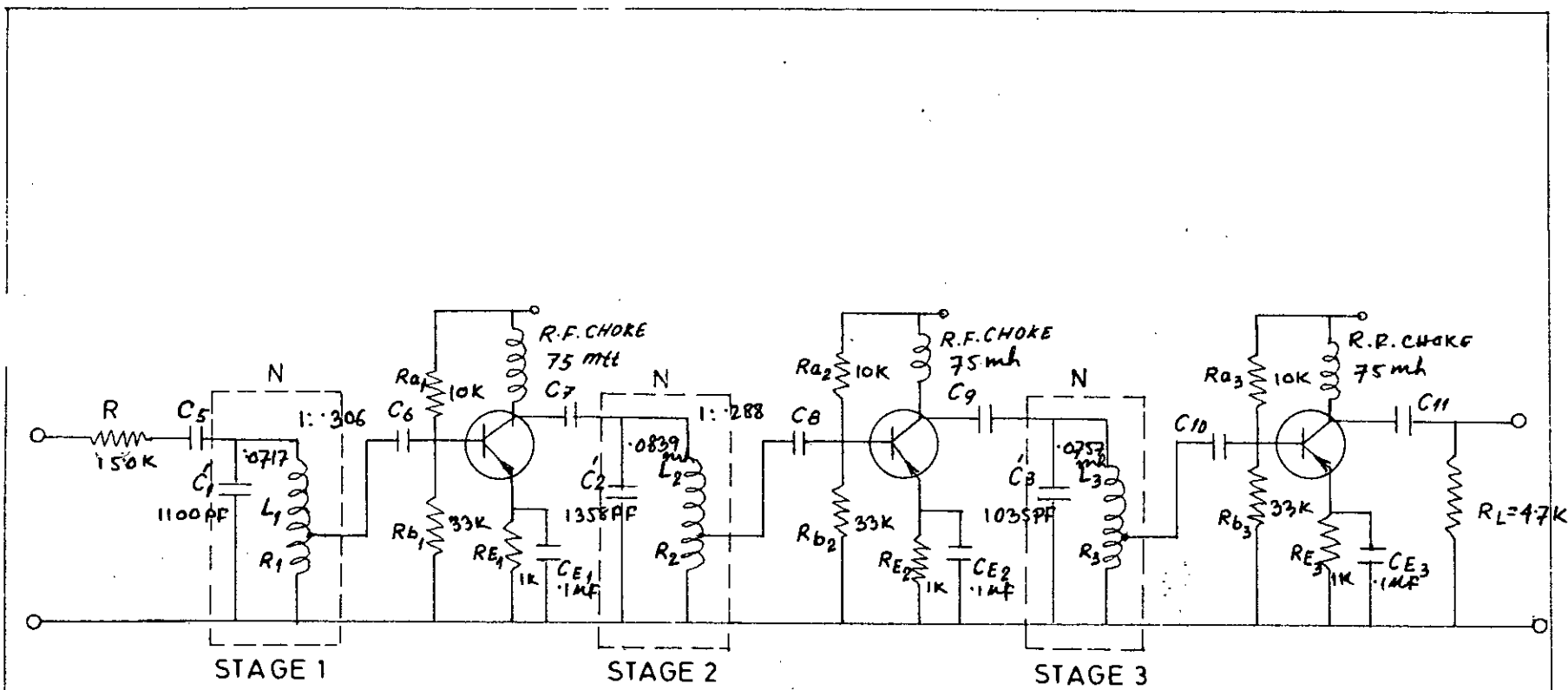
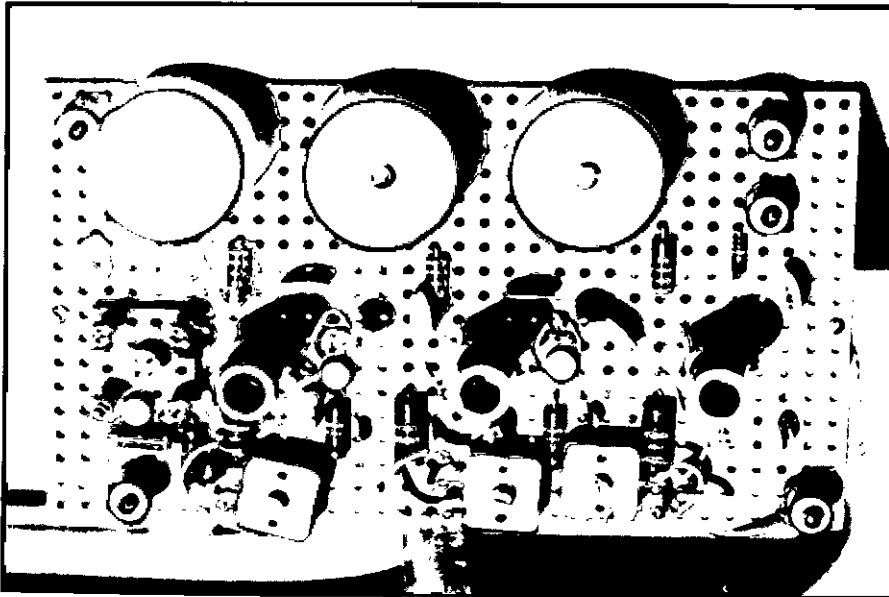


FIG. 4-1A ACTUAL FILTER CIRCUIT



**Photograph of The Filter Circuit
(Single Tuned Interstage)**

4.6 Comparison of measured Frequency Response Characteristics with Theoretical Characteristics.

The programme used to determine the theoretical frequency response characteristic $\text{Im} Z_{12}(s)$ (Eqn. 4.5) is given in Appendix C. The result thus obtained is plotted in fig. 4.8 (Curve 1).

The designed filter circuit (fig.4.1) was constructed and its performance was measured by measuring input current and output voltage for the corresponding frequencies.

The result is given in table 4.1. The frequency response curve is plotted (frequency vs. normalized gain) in fig. 4.8 (curve II). Normalized gain in db vs. frequency is plotted in fig. 4.9 both theoretical and measured case.

Comparing the theoretical and measured performance of the filter, we observe that

	f_0 in KHz	Nb.of ripple	Bandwidth in KHz	Gain at band edges in db	Gain at 500 KHz in db.
Theoretical	455	3	40	-3	-26
Measured	455	3	40	-3	-17.2

Though attenuation at 500 KC for practical case is much less than that of the theoretical case, but it still meets the specification (-15 db). Therefore, we can conclude that practical result is quite satisfactory, though ripple in the practical case is not exactly equal but they are within the limit of $\frac{1}{2}$ db. as per specification.

TABLE- 4.2

Frequency in KHz	Input voltage V_1 (peak to peak) in volts	Input current (Peak to peak) $I_{in} = \frac{V_{in}}{150 \times 10^3}$ mA	Output voltage (Peak to peak) in volts.	Gain $F(\omega) = \frac{V_{out}}{I_{in}}$ $\times 10^6$	Normal- ized gain $\frac{F(\omega)}{F(\omega)_{455}}$	Normal- ized gain in DB
400	1.0		0.22	0.033	0.038	-28.40
405	1.0		0.30	0.045	0.0517	-24.75
410	1.0		0.45	0.0675	0.0776	-22.20
415	1.0		0.65	0.0975	0.112	-19.00
420	1.0		1.0	0.150	0.173	-15.28
422.5	1.0		1.40	0.210	0.241	-12.32
425	1.0		1.70	0.255	0.293	-10.66
427.5	1.0		2.10	0.315	0.363	-8.82
430	1.0		2.60	0.390	0.450	-6.92
432.5	1.0		3.20	0.478	0.550	-5.16
435	1.0	6.67	4.30	0.600	0.710	-3.00
437.5	1.0		5.55	0.825	0.950	-0.44
440	2.0		5.80	0.870	1.00	-0.0
442.5	1.0		5.90	0.880	1.01	0.06
445	1.0		5.75	0.862	0.99	-0.08
447.5	1.0		5.65	0.847	0.97	-0.26
450	1.0		5.60	0.840	0.965	-0.30
452.5	1.0		5.70	0.845	0.975	-0.24
455	1.0		5.80	0.870	1.00	00
457.5	1.0		5.75	0.855	0.98	-0.16
460	1.0		5.65	0.847	0.97	-0.26
462.5	1.0		5.65	0.847	0.97	-0.26
465	1.0		5.70	0.855	0.98	-0.16
467.5	1.0		5.80	0.870	1.00	-0.0
470	1.0		5.90	0.880	1.01	0.06
472.5	1.0		5.55	0.825	0.95	-0.44
475	1.0		4.30	0.60	0.71	-3.00
477.5	1.0		3.75	0.565	0.650	-3.52
480	1.0		3.50	0.525	0.605	-4.32
482.5	1.0		3.00	0.450	0.515	-5.76
485	1.0		2.40	0.360	0.400	-7.96
487.5	1.0		1.75	0.260	0.298	-10.20
490	1.0		1.60	0.240	0.276	-11.16
495	1.0		1.10	0.165	0.190	-14.40
500	1.0		0.80	0.120	0.138	-17.20
505	1.0		0.60	0.090	0.104	-19.64
510	1.0		0.45	0.0675	0.0775	-22.00
515	1.0		0.35	0.0525	0.060	-24.40

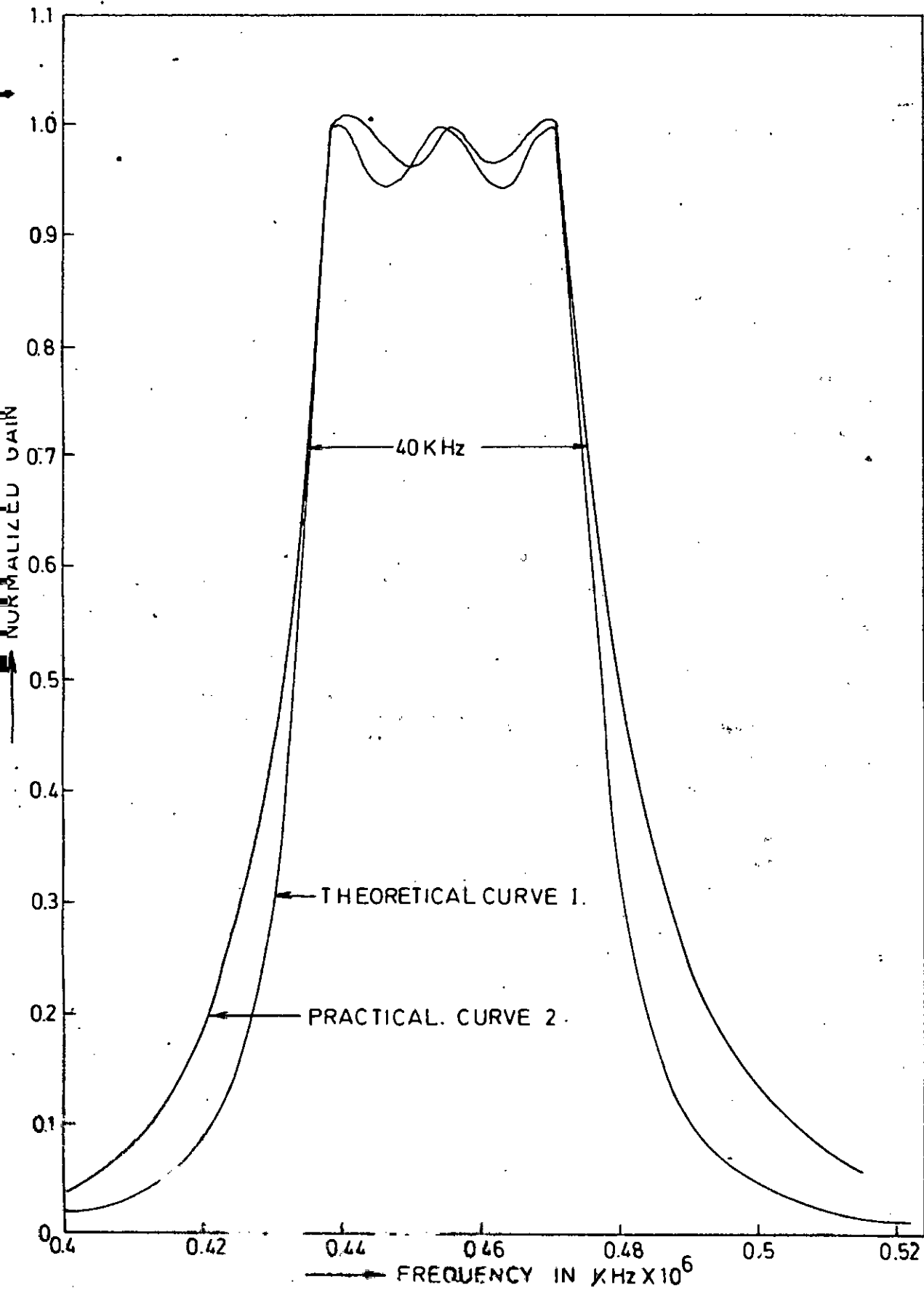


FIG. 4.8 FREQUENCY RESPONSE CHARACTERISTIC

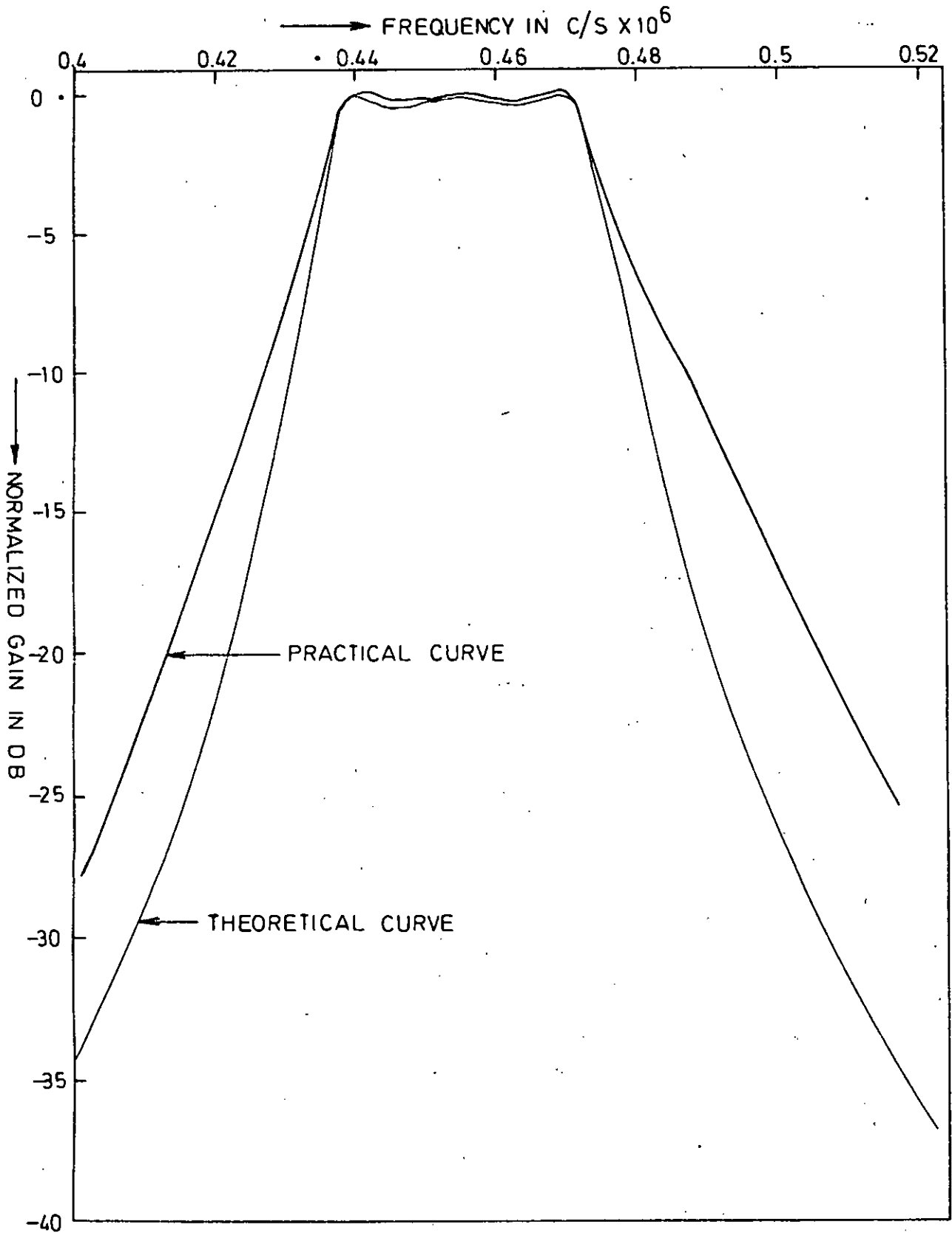


FIG. 4.9 NORMALIZED GAIN IN DB Vs. FREQUENCY

CHAPTER-5

ACTIVE FILTER DESIGN WITH DOUBLE TUNED INTERSTAGE :

This chapter provides an example of transistor amplifier design with three interstages when the response of the amplifier was prescribed, using the second method discussed in chapter-3.

5.1 Specification of amplifier response:

It is required to design a bandpass filter with \pm db. tolerance in the passband, having centre frequency $f_0 = 455$ KHz, 3 db bandwidth 40 KHz. Also the magnitude of the transfer function must be at least 20 db down at $f_x = 485$ KHz from its value at the centre frequency.

Determination of transfer function for lowpass response.

We will have to calculate n for the required magnitude characteristic which will determine the number of poles of the transfer function.

Given points are,

Centre frequency, $f_0 = 455$ KHz.

Bandedges are $f_2 = 475$ KHz.

$f_1 = 435$ KHz.

Magnitude condition is given at $f_x = 485$ KHz.

The corresponding points in the low-pass magnitude characteristic can be obtained using the frequency transformation given by the relation of eqn.(2.39).

These points are :

Points in bandpass	Corresponding pts. in lowpass.
j455 KHz	0
j475 KHz	j1
j435 KHz	-j1
j485 KHz	j1.4

The lowpass Chebyshev characteristic is represented by the expression

$$|T_{12}|^2 = (1/(1 + \epsilon^2 C_n^2(\omega)) \theta$$

For $\frac{1}{2}$ db ripple, $\epsilon = 0.2434$, $\epsilon^2 = 0.0593$.

Since the magnitude characteristic remains unchanged by the frequency transformation, we can write as required by the specification

$$\begin{aligned} 1/(1 + \epsilon^2 C_n^2(1.4)) &= 10^{-2} \\ \text{or, } 1 + \epsilon^2 C_n^2(1.4) &= 100. \\ \text{or } C_n(1.4) &= 40.8 \quad - (A) \end{aligned}$$

But $C_n(\Omega) = 2^{n-1} \Omega^n$ retaining only the first term Chebyshev polynomial.

With $n=5$

$$C_5(1.4) = 20.6$$

With $n=6$

$$C_6(1.4) = 41.$$

Therefore, $n=6$ meets the specification.

For $n=6$, lowpass Butterworth poles are :

$$\begin{aligned} P'_1 &= -0.96593 \pm j0.25882 \\ P'_2 &= -0.70711 \pm j0.70711 \\ P'_3 &= -0.25882 \pm j0.96593 \end{aligned} \quad \text{-----(5.1).}$$

and the corresponding lowpass Chebyshev poles with $\frac{1}{2}$ db. ripples ($\epsilon^2 = 0.0593$, $\epsilon = 0.2434$) are :

$$\begin{aligned} P_1 &= -0.32707 \pm j0.25882 \\ P_2 &= -0.24001 \pm j0.70711 \\ P_3 &= -0.08705 \pm j0.96593 \end{aligned} \quad \text{-----(5.2).}$$

The lowpass transfer function now becomes

$$Z_{12}(p) = \frac{1}{(p-p_1)(p-\bar{p}_1)(p-p_2)(p-\bar{p}_2)(p-p_3)(p-\bar{p}_3)} \quad \text{-----(5.3).}$$

5.2- Determination of bandpass poles and zeros.

The poles given in eqn. (5.2) are now transformed by lowpass to bandpass transformation, eqn. (2-40) and (2.41).

Here $B = f_2 - f_1 = 40 \text{ KHz.}$

$f_2 = 475 \text{ KHz}$

$f_1 = 435 \text{ KHz.}$

$f_0 = \sqrt{f_1 f_2}$

Using the programme in Appendix B, we have the required poles (normalized by $2\pi \times 10^6$) and given below.

$s_1 = -0.00168 + j0.43568$

$s_2 = -0.00465 + j0.44061$

$s_3 = -0.00648 + j0.44936$

$s_4 = -0.00663 + 0.49972$

$s_5 = -0.00495 + j0.46890$

$s_6 = -0.00183 + j0.472247420.$

----- (5.4)

Therefore in the bandpass case, the transfer function is

$$Z_{12}(s) = \frac{s^6}{(s-s_1)(s-\bar{s}_1)(s-s_2)(s-\bar{s}_2)(s-s_3)(s-\bar{s}_3)(s-s_4)(s-\bar{s}_4)(s-s_5)(s-\bar{s}_5)(s-s_6)(s-\bar{s}_6)} \quad \text{----- (5.5)}$$

of 12 zeroes, six are at the origin and the other six at infinity. This transfer function meets the design specification. The interstages N_i of fig.3.2 have to be so designed that the amplifier gives the same response as that of the transfer function of eqn.(5.5).

5.3 Detailed consideration of a typical stage:

Fig. 3-2 with biasing elements is shown in fig. 5.1. The tapings are used for impedance matching purpose. The equivalent circuit is shown in fig. 5.2.

Now consider a typical stage such as stage 3 of fig. 5.2 and is redrawn in fig. 5.3.

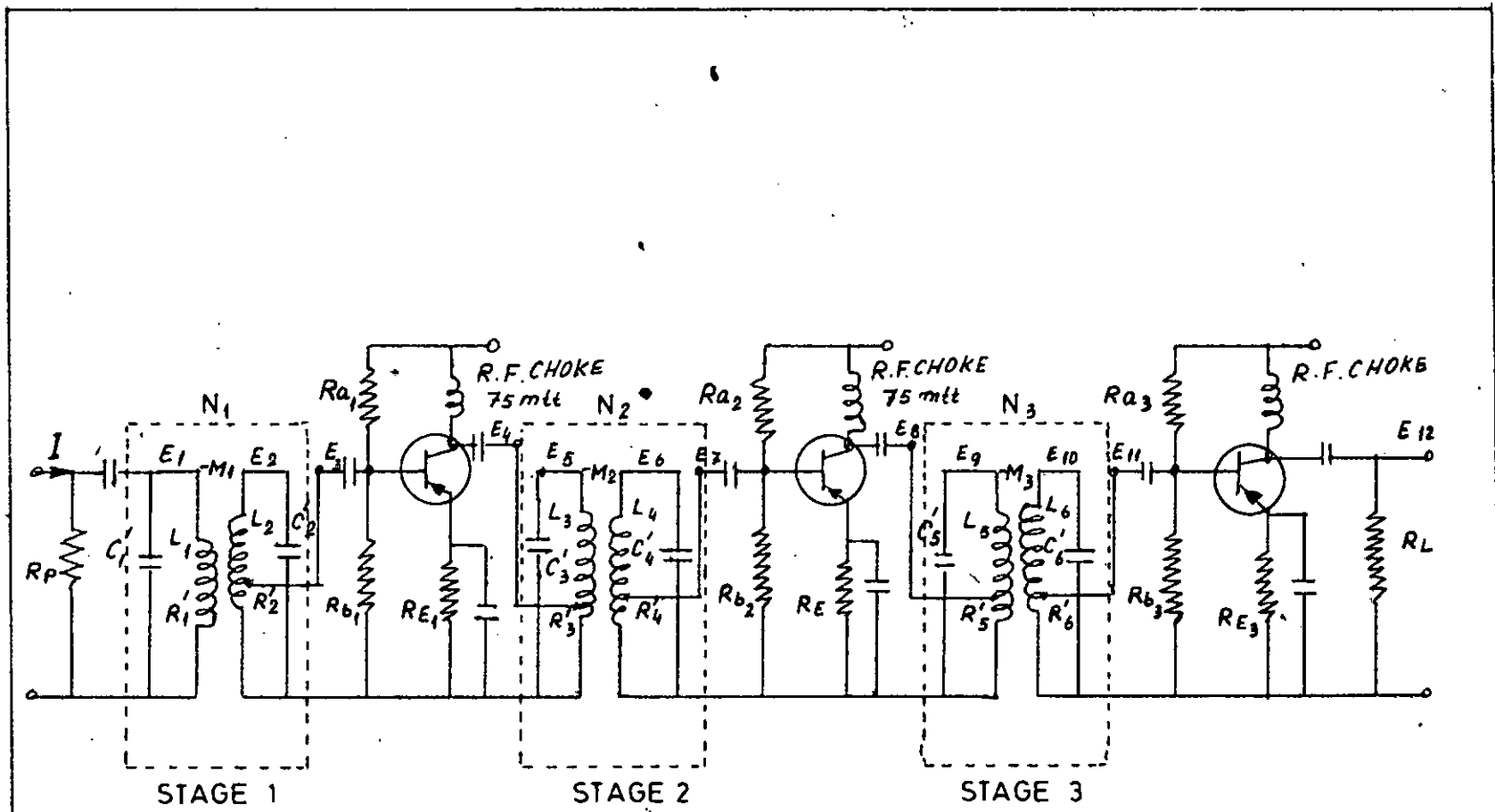


FIG. 5.1 THREE STAGE DOUBLE TUNED FILTER CIRCUIT

No. 1 (12) Cap...

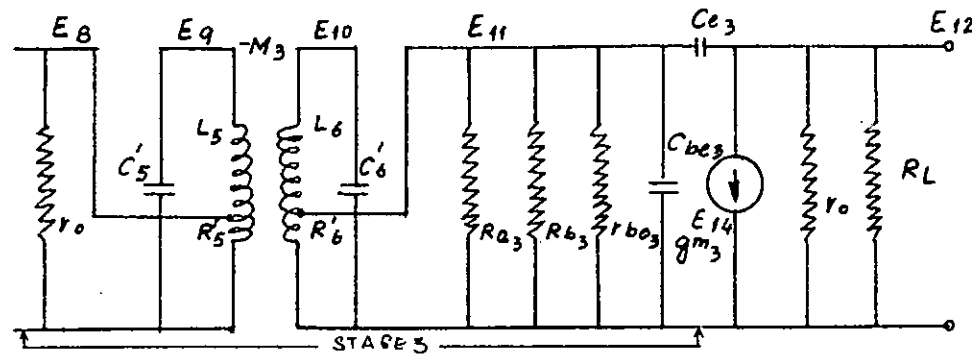
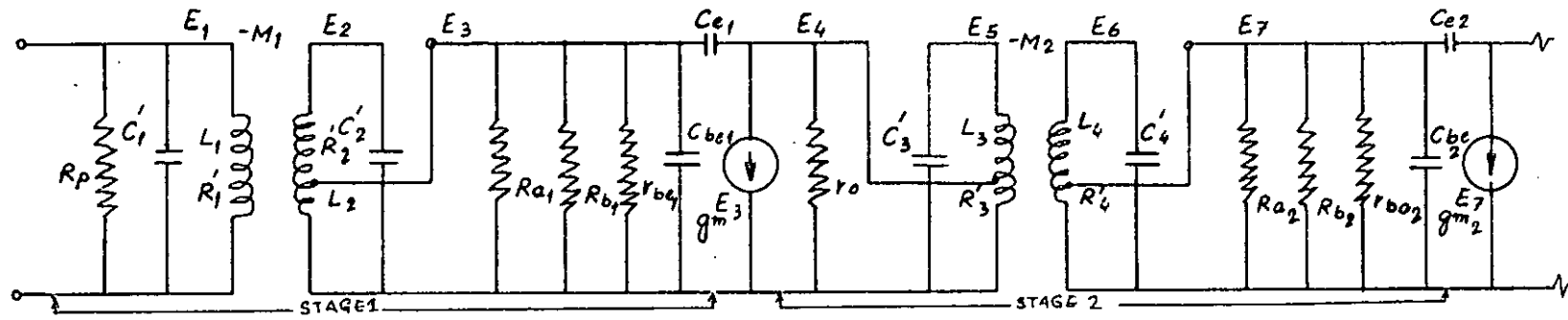


FIG. 5.2 EQUIVALENT CIRCUIT OF FIG. 5.1

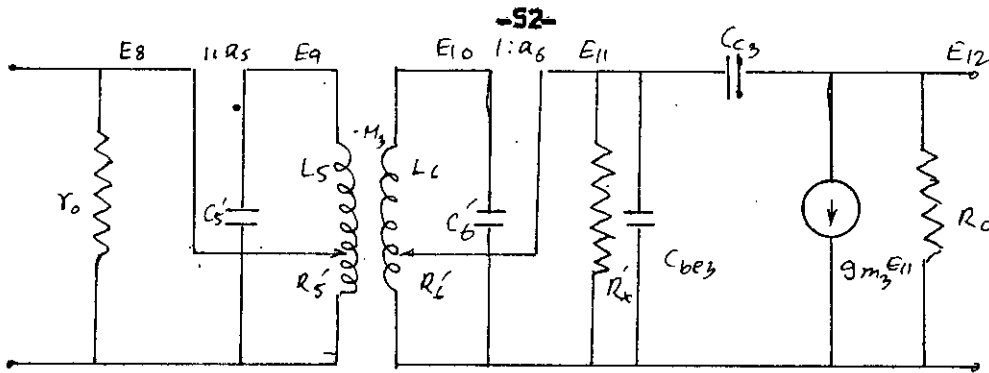


Fig. 5-3. A stage of the filter circuit of fig. 6.1.

Where $R'_x = R_{e3} \parallel R_{b3} \parallel r_{be3}$

$$R_0 = \frac{r_0 R_L}{r_0 + R_L}$$

The equivalent circuit of fig. 5.3 can be simplified by applying Miller effect and is shown in fig. 5.4.

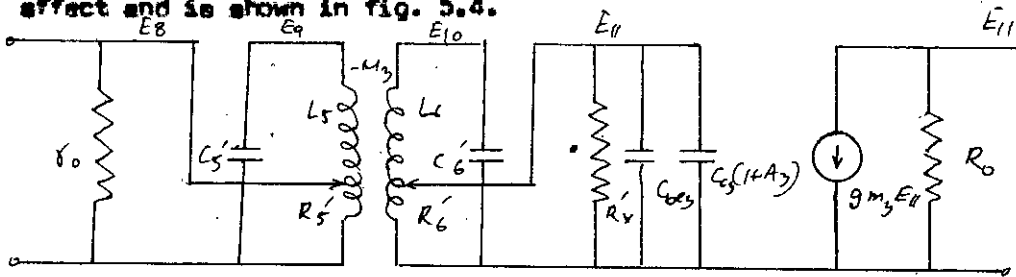


Fig.5.4. The typical stage of fig. 5.1 simplified using miller effect.

Where $A_3 = g_{m3} R_0$ (5.6).

The circuit of fig. 5.4 can further be simplified to the circuit shown in fig.5.5, with the following expression.

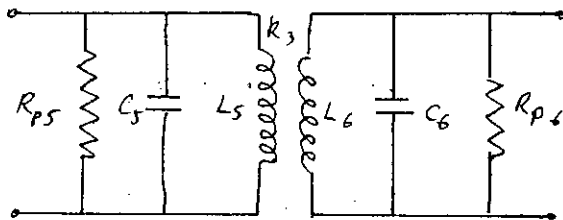


Fig. 5.5. Simplified form of the stage of fig. 5.3.

Where $a_6 = E_{11} / E_{10}$

$a_5 = E_9 / E_8$

$$1/R'_x = 1/R_{e3} + 1/R_{b3} + 1/x_{be3}$$

$$R_{p6} = R'_x / a_6^2 \parallel R'_{p6}$$

$$R'_{p6} = L_6 / C_6 R'_6$$

----- (5.7)

R'_6 = series resistance of the inductance L_6

$$R_6 = L_6 / C_6 R_{p6}$$

$$C_6 = C'_6 + a_6^2 [C_{be3} + C_{c3} (1 + A_3)]$$

$$A_3 = a_{m3} x_o R_L / (x_o + R_L)$$

$$R_{p5} = a_5^2 x_o \parallel R'_{p5}$$

$$R'_{p5} = L_5 / C_5 R'_5$$

R'_5 = series resistance of the inductance L_5

$$R_5 = L_5 / C_5 R_{p5}$$

This simplified stage resembles the interstage network of fig. 3.14. It was shown that this stage can be used to realize two pair of poles and four zeros unevenly distributed between the origin and infinity, as a result this circuit does not provide with symmetrical frequency response characteristic, if the pole location are unchanged. To have symmetrical frequency response, the origin pole locations (eqn.5.4) must be adjusted by an appropriate method.

The value of parameters of fig. 5.5 realizing two pair poles and four zeros can be obtained from the simultaneous solution of the non-linear equations (3.32). The value of biasing elements and transistor parameters depend on the operating point. Therefore, the quiescent point and the values of a_6 and a_5 must be selected in such a way that all the parameters become positive. To meet these requirements, few trials may be required.

For stages 2 & 1 exactly similar equations are obtained.

5.4 Adjustment of pole location for symmetrical frequency response characteristic.

In this section we want to adjust the pole location in such a way that the specification of passband tolerance is met with unequal division of the zeros between the origin and infinity.

Curve I of fig. 5.6 is a plot of the frequency response of a filter circuit, desired response, with pole locations given by eqn.(5.4) and with 6 zeros at origin and six at infinity. Curve II of fig. 5.6 is a plot of the frequency response that would have been realized for the same pole location and with 3 zeros at origin and nine at infinity.

In a multipole transfer function, the peaks of the frequency response occur at frequencies which are the imaginary part of pole positions and the magnitude of the peaks depend on the corresponding real part of the poles.

From the curves I and II of fig. 5.6, it is evident that the pole locations for curve II must be shifted in order to reduce the error between ideal and the actual curve. Since peaks of both the curves occur at the same frequency, we may consider the imaginary parts of the poles as constant. As we have to reduce the magnitude of the curve II left of the centre frequency f_0 , the real parts of the poles located in this region are to be increased while to increase the magnitude of the curve II right of the centre frequency f_0 , magnitude of the real parts of the poles in this region are to be decreased. In general, poles left of the centre frequency are to be shifted away from the imaginary axis while the other poles are to be shifted towards the imaginary axis.

The programme used to find the adjusted poles is given in appendix D. After a few trials, the pole location (normalized by $2^n \times 10^6$) were found to be

$$\begin{aligned} S_1 &= -0.00181 + j0.43565. \\ S_2 &= -0.00511 + j0.44061. \\ S_3 &= -0.00666 + j0.44936 \\ S_4 &= -0.00647 + j0.43972 \quad \dots\dots\dots(5.8). \\ S_5 &= -0.00460 + j0.46890 \\ S_6 &= -0.00161 + j0.47428 \end{aligned}$$

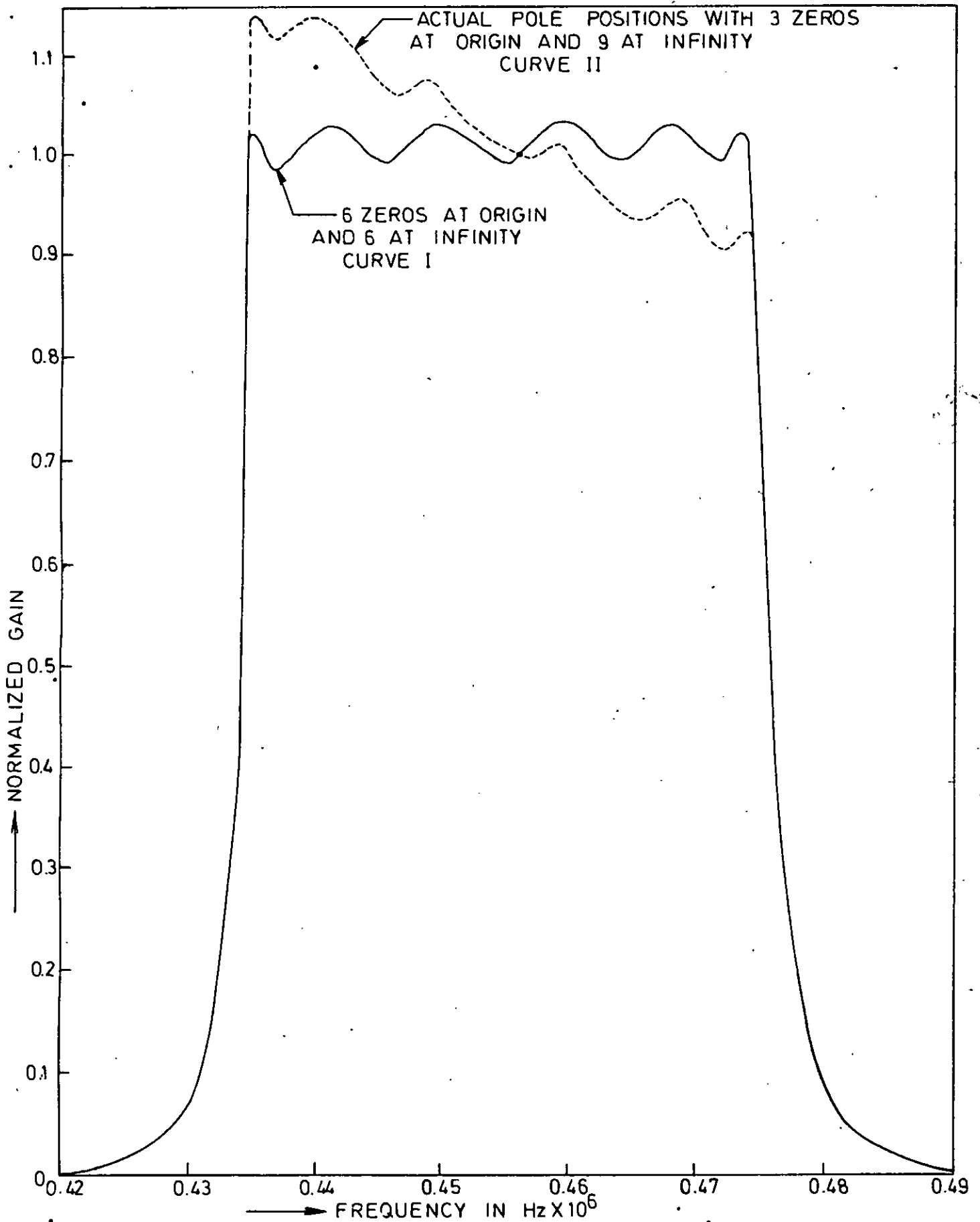


FIG. 5-6 FREQUENCY RESPONSE CHARACTERISTIC

These gave the same frequency response as shown by curve 1 of fig. 5.6.

5.5 Determination of values of parameters for each interstage

From the pole positions given by eqn. (5.8), we can readily obtain the element values of the three interstage networks of figs. 5.1 realizing two pair of poles by each stage. The element values can be calculated by solving the simultaneous non-linear eqns. (3.29) of chapter 3.

A programme used to solve these is given in Appendix E.

Stage 3

To determine the quiescent current, D.C. parameters and transistor network parameter, we consider the emitter current $I_E = 0.75 \text{ mA}$ and supply voltage $E_{DC} = 6V$.

$$\text{Base current} = I_C / \beta = I_E / \beta = 12.5 \mu A$$

$$\text{Let the bleed current be } 132.5 \mu A$$

$$\text{Current flowing through } R_{e3} = 144 \mu A$$

$$\text{Let the voltage across } R_E = 1.125 \text{ V.}$$

$$R_{E3} = 1.125 / I_E = 1.5 \text{ K.}$$

$$\text{Therefore voltage across } R_{b3} = 1.325 \text{ V.}$$

$$R_{b3} = 1.325V / 132.5 \mu A \approx 10 \text{ K.}$$

$$\text{Voltage across } R_{e3} = E_{DC} - 1.325 \text{ V} = 4.675 \text{ V.}$$

$$R_{e3} = 4.675 \text{ V} / 144 \mu A \approx 33 \text{ K.}$$

From eqn. (4.13)

$$E_1 = 1.395 \text{ V.}$$

$$R_1 = 7.61 \text{ K.}$$

From eqn. (4.16)

$$I_C = 0.74 \text{ mA.}$$

$$\beta = 80 \text{ for 2N1683 transistor.}$$

For 2N1683 transistor:

$$f_T = 50 \text{ MHz}, h_{fe} = 80, h_{re} = 3.36 \times 10^{-4}, C_c = 12 \text{ pf.}$$

$$g_{m3} = 0.0296 \text{ mho.}$$

$$r_{ba3} = 2.7k$$

$$r_o = 100k$$

$$C_{be3} = 94.2 \text{ pf.}$$

Let this stage realize the poles S_2 and S_5 of eqn.(5.8). The solution of eqn. (3.32) gives the following values.

$$R_6/L_6 = 0.70215 \times 10^5 \quad \text{-----(5.9)}$$

$$1/L_6 C_6 = 0.70489 \times 10^5 \quad \text{-----(5.10)}$$

$$R_5/L_5 = 0.515 \times 10^5 \quad \text{-----(5.11)}$$

$$1/L_5 C_5 = 0.84566 \times 10^{13} \quad \text{-----(5.12)}$$

$$K_3 = 0.05$$

Secondary side

$$A_3 = 109 \text{ where } R_2 = 6.8k.$$

For $L_6 = 0.204 \text{ mh}$, we have $R'_{p6} = 36k$ at 455 KHz.

From eqn. (5.9)

$$R_6 = 14.3 \Omega$$

From eqn. (5.10)

$$C_6 = 630 \text{ pf}$$

$$R_{p6} = 22.8 k.$$

$$R_{p6} = R'_x / s_6^2 \parallel R'_{p6} \quad \text{-----(5.13)}$$

$$R'_x = 2 k.$$

From eqn. (5.13)

$$s_6 = 0.18$$

$$R'_6 = 9 \Omega$$

Total capacitance from the next stage

$$C_{E3} = 77 \text{ pf.}$$

$$C'_6 = C_6 - C_{E3} = 353 \text{ pf.}$$

Primary side

$$\text{for } L_5 = 0.2 \text{ mh, } R'_{p5} = 42\text{K at } 455 \text{ KHz.}$$

From eqn. (5.11)

$$R_5 = 10.3 \Omega$$

From eqn. (5.12)

$$C_5 = 590 \text{ pf.}$$

$$C'_5 = C'_5 = 590 \text{ pf.}$$

$$R_{p5} = 32.0 \text{ K.}$$

R_{nt}

$$a_5 = 1.22$$

$$R'_5 = k 8.07 \Omega$$

Stage 2

For the same operating point as stage 3, the d.c. parameters and transistor parameters have the values as calculated for stage 3.

This stage realizes the poles S_3 and S_6 of eqn. (5.6) for which the solution of eqn. (3.32) gives.

$$R_4/L_4 = 0.83910 \times 10^5 \text{ -----(5.14)}$$

$$1/L_4 C_4 = 0.79734 \times 10^{13} \text{ -----(5.15)}$$

$$R_3/L_3 = 0.2 \times 10^5 \text{ -----(5.16)}$$

$$1/L_3 C_3 = 0.86703 \times 10^{13} \text{ -----(5.17)}$$

$$k_2 = 0.01$$

Secondary side

$$A_2 = \frac{g_{m3} R_{p5}}{a_5^2} \quad F_0 = 646$$

$$\text{for } L_4 = 0.197 \text{ mh, } R'_{p4} = 33.6\text{K at } 455 \text{ KHz.}$$

From eqn. (5.14)

$$R_4 = 16.5 \Omega$$

From eqn. (5.15)

$$C_4 = 635 \text{ pf.}$$

$$R_{p4} = L_4 / C_4 R_4 = 19 \text{ K.}$$

Let a 270K resistor is inserted in the secondary side.

$$R'_{p4} = 270 \text{ k} \parallel R'_{p4} = 30 \text{ K.}$$

$$R_{p4} = R'_x / a_4^2 \parallel R'_{p4} = 19 \text{ K}$$

$$R'_x = 2 \text{ K.}$$

$$a_4 = 0.197.$$

$$R'_4 = 9.24 \Omega$$

Total capacitance from the next stage

$$C_{t2} = 300 \text{ pf.}$$

$$C'_4 = C_4 - C_{t2} = 335 \text{ pf.}$$

Primary side

$$\text{For } L_3 = 0.2 \text{ mh, } R'_{p3} = 72 \text{ K.}$$

From eqn. (5.16)

$$R_3 = 4 \Omega$$

From eqn. (5.17)

$$C_3 = 600 \text{ pf.}$$

$$R_{p3} = 75 \text{ K.}$$

$$R'_3 = 4.1 \Omega$$

In order to eliminate the shunting effect of r_o on this primary side, $a_3 = 2.74$ is taken.

For stage 1

The operating point of this stage is same as the other two stages and it realizes the poles s_1 and s_4 of eqn. (5.8) for which the solution of eqn.(3.32) gives

$$R_1/L_1 = 0.0004 \times 10^9 \text{ ----- 5.18.}$$

$$1/L_2 C_2 = 0.8362 \times 10^{13} \quad \text{-----(5.19).}$$

$$R_1/L_1 = 0.24 \times 10^5 \quad \text{-----(5.20)}$$

$$1/L_1 C_1 = 0.7474 \times 10^{13} \quad \text{-----(5.21)}$$

$$K = 0.01.$$

Secondary side

$$A_1 = 157$$

For $L_2 = 0.197$ mh, $R'_{p2} = 34$ K at 455 KHz.

From eqn. (5.18).

$$R_2 = 15.76 \Omega$$

From eqn. (5.19)

$$C_2 = 610 \text{ pf.}$$

$$R_{p2} = 20.7 \text{ K.}$$

$$R_{p2} = R''_x / a_2^2 \quad || \quad R'_{p2} = 20.7 \text{ K}$$

$$R''_x = 2 \text{ K.}$$

$$a_2 = 0.194.$$

$$R'_2 = 9.5 \Omega$$

Total capacitance from the next stage

$$C_{t1} = 77.5 \text{ pf.}$$

$$C'_2 = C_2 - C_{t1} = 532.5 \text{ pf.}$$

Primary side

For $L_1 = 0.203$ mh, $R'_{p1} = 60$ K.

From eqn. (5.20)

$$R_1 = 4.87 \Omega$$

From Eqn. (5.21)

$$C_1 = 660 \text{ pf.}$$

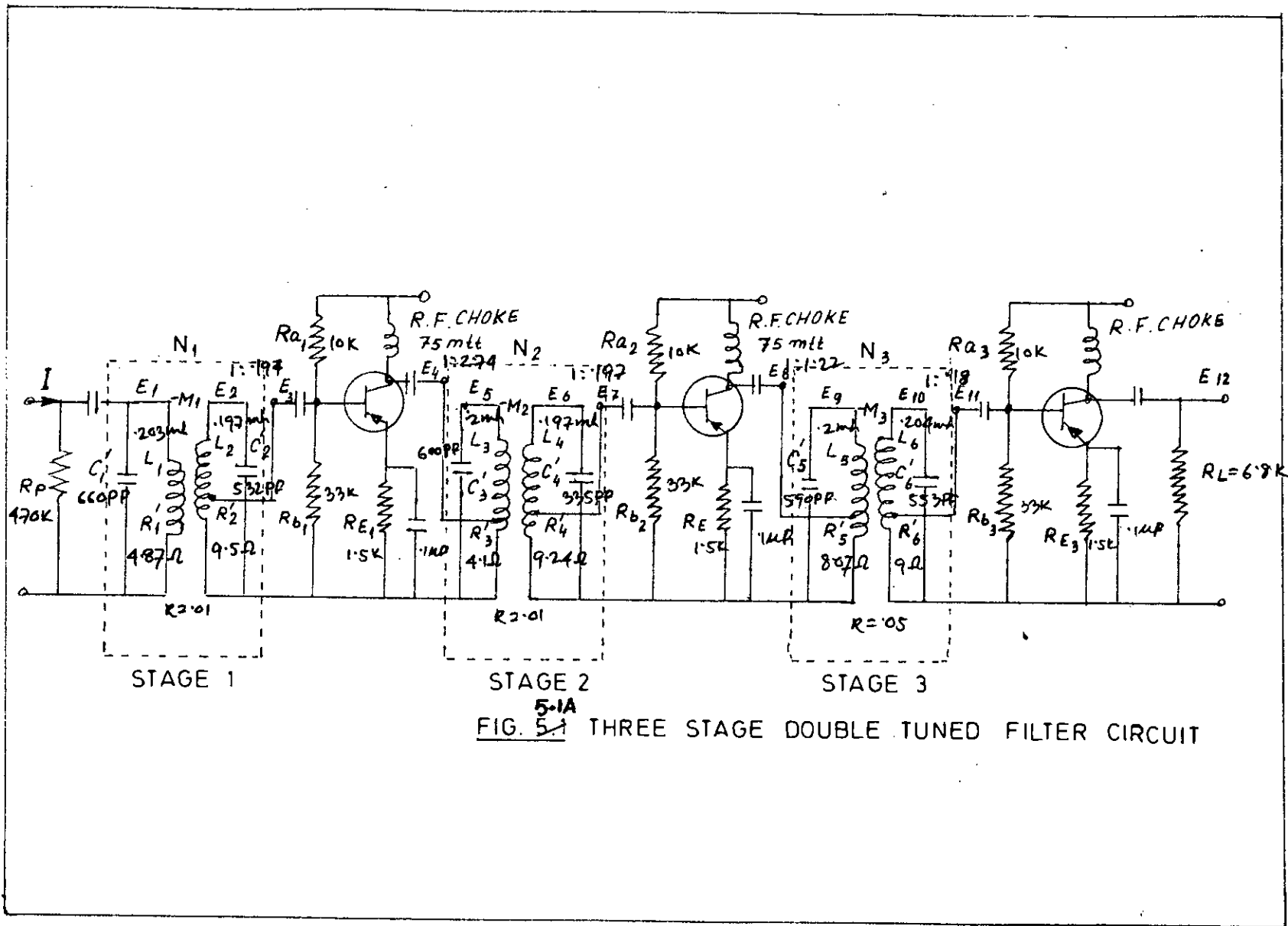
$$C_1 = C'_1$$

$$R_p = 680 \text{ K}$$

$$R_{o1} = 62 = R'_{p1}$$

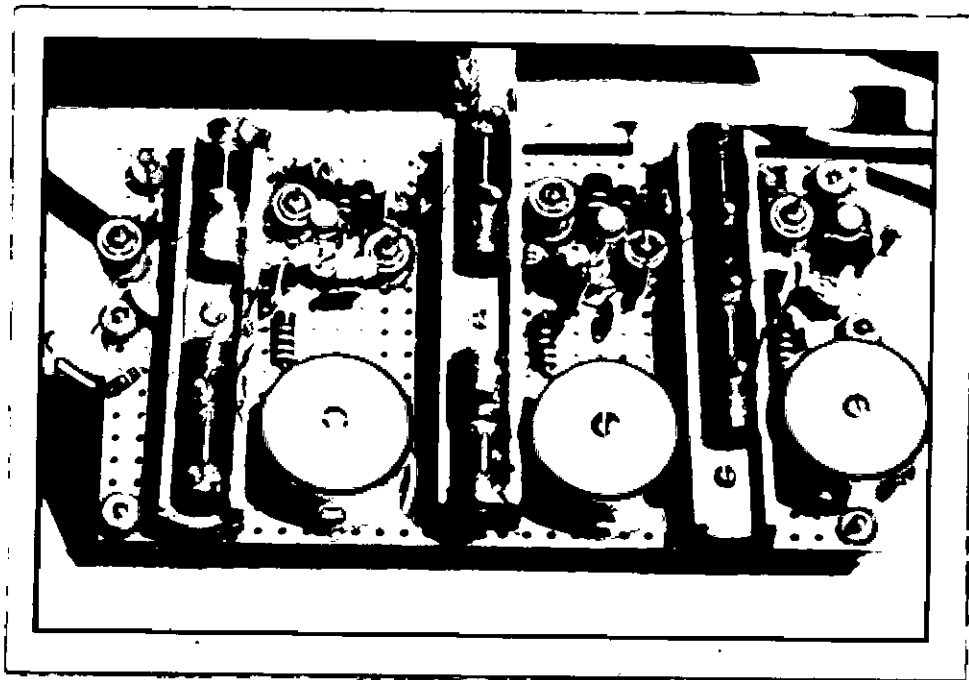
$$R'_1 = 4.87 \Omega$$

Calculated parameter values are shown in the attached circuit (Fig 5.1A)



5.1A
 FIG. 5.1 THREE STAGE DOUBLE TUNED FILTER CIRCUIT

No. 112/424



Photograph of The Filter Circuit
(Double Tuned Interstage)

5.6 Some Comparison of Measured Frequency Response Characteristic with Theoretical Characteristic.

The programme in Appendix C is used to determine the theoretical frequency response characteristic for poles of eqn. (5.8) and the result is plotted in fig. 5.7 (Curve 1).

The designed filter circuit was constructed and its frequency response characteristic is determined by measuring input current and output voltage for the corresponding frequencies. The result is given in table 5-1.

The frequency response characteristic is plotted in fig. 5.7 (Curve II). Comparing the curves of fig. 5.7, we observe that

	f in KHz	Bandwidth in KHz	Gain at band edges in db.	Gain at 485 KHz in db.
Theoretical	455	40	-3	-34.54
Measured	455	40	-3	-21.2

Attenuation at 485 KHz for practical case is much less than that of theoretical case, but it meets the specification (-20 db). In practical case ripples are not exactly equal as theoretical case, but they are within the limit of $\frac{1}{2}$ db. and also number of ripples in the practical case is less than that of the theoretical because of the coincidence of some of peaks due to non-availability of high Q-coils.

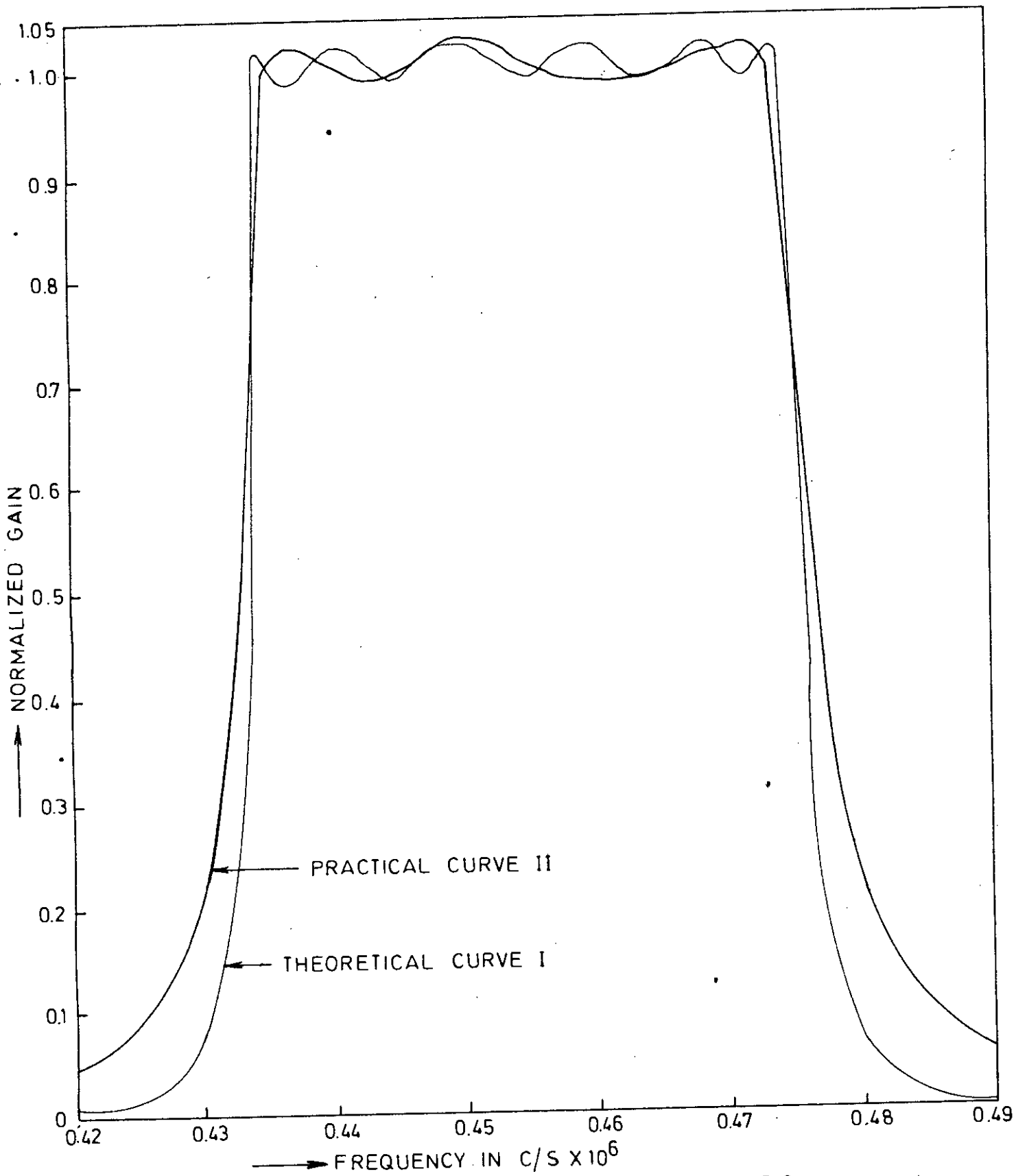


FIG. 5.7 FREQUENCY RESPONSE CHARACTERISTIC

TABLE- 5.1

Frequency in KHz	Input voltage V_1 (Peak to peak) in volts	Input current (Peak to peak) $I_{in} =$ $\frac{V_{in}}{470K}$ in A	Output voltage (Peak to peak) in volts	Gain $F(\omega) =$ $\frac{V_{out}}{I_{in}}$ $\times 10^6$	Normali- zed gain: $\frac{F(\omega)}{F(\omega)_{455}}$
400	0.40	8.51	0.0	0.0	0.0
410	0.40	8.51	0.024	0.0247	0.03
420	0.40	8.51	0.035	0.0417	0.05
425	0.40	8.51	0.06	0.0705	0.0855
430	0.40	8.51	0.165	0.194	0.235
432.5	0.40	8.51	0.37	0.435	0.527
435.0	0.40	8.51	0.70	0.825	1.00
437.5	0.40	8.51	0.715	0.840	1.020
440	0.40	8.51	0.70	0.825	1.00
442.5	0.40	8.51	0.690	0.810	0.98
445	0.40	8.51	0.70	0.825	1.00
447.5	0.40	8.51	0.71	0.835	1.01
450	0.40	8.51	0.72	0.843	1.03
452.5	0.40	8.51	0.72	0.845	1.03
455	0.40	8.51	0.70	0.825	1.00
457.5	0.40	8.51	0.695	0.818	0.992
460	0.40	8.51	0.690	0.810	0.980
462.5	0.40	8.51	0.695	0.818	0.992
465.0	0.40	8.51	0.70	0.825	1.00
467.5	0.40	8.51	0.70	0.825	1.00
470	0.40	8.51	0.71	0.835	1.01
472.5	0.40	8.51	0.715	0.840	1.02
475	0.40	8.51	0.480	0.577	0.70
477.5	0.40	8.51	0.275	0.324	0.392
480	0.40	8.51	0.17	0.198	0.24
485	0.40	8.51	0.055	0.0647	0.0785
490	0.40	8.51	0.042	0.0495	0.06
500	0.40	8.51	0.028	0.033	0.005

CHAPTER-6

SUMMARY, CONCLUSION AND FURTHER WORK

Synthesis procedures have been given for interstage networks of an active bandpass filter, the frequency response characteristic of which is a close approximation of the ideal characteristics and which provides equiripple in the passband and maximum sharpness outside the passband.

In chapter 2, Butterworth and Chebyshev polynomials are used to approximate the ideal lowpass transfer function to obtain a realizable rational transfer function that satisfies the given specification. This chapter also gives procedures for transforming lowpass specification to bandpass and vice versa.

In chapter 3, it is shown that if each transistor can be assumed to be resistively loaded within the desired frequency range, then with the application of Miller effect, the transistor amplifier can be divided into electrically similar sections, called the interstages. It has been established that the transfer function of the amplifier is simply the product of the transfer function of all individual interstages. This chapter also provides two methods of synthesizing interstage networks for a multistage transistorized filter to achieve bandpass response. The first method deals with synthesizing each interstage that must realize a certain number of poles and zeros of the over-all transfer function that achieve the prescribed response. The second one deals with synthesizing an interstage of preselected configuration to achieve the prescribed response.

In chapter 4, interstage networks realizing one pair of poles and two zeros of over-all transfer function per stage have been designed, obtaining the interstage network in the form of single tuned circuit. The parameters of each interstage have been evaluated from the positions of the transformed Chebyshev poles and zeros that have been assigned to this stage for realization. A prototype of the filter has been constructed and measurements have been made to determine its frequency response characteristics.

A comparison of the ideal and the measured response shows that measured characteristics of the amplifier closely resembles the predicted response. However it is observed that passband ripples in the two cases are not same and the rate at which

the magnitude characteristics falls off outside the passband is less than that of the ideal case, but it meets the design specification. This is not unexpected, as many of the assumptions that were made to simplify the circuit model of the transistor are only approximate.

These assumptions are : Miller effects in simplifying the transistor models, load offered by a stage to the proceeding stage is considered to be resistive and constant at the tuned frequency value of the respective circuit, 5% and 10% tolerable resistors are in use, etc.

It is seen that a single tuned circuit can be used to realize a pair of conjugate poles and two zeros. But to increase the sharpness outside the passband, increased number of poles and zeros are to be realized. To realize increased number of poles and zeros using single tuned circuit, one has to increase number of stages which economically may not be feasible. But increased number of poles and zeros can be realized without increasing the number of stages by the use of double tuned circuit.

Analysis and design procedures for interstages in the form of double tuned circuits have been given in chapter 5. Analysis of a double tuned circuit shows that it can be used to realize two pair of poles (including complex conjugates) and four zeros. It has been found that, when designed to realize chebyshev poles for bandpass response, the amplifiers with double tuned interstages do not display symmetrical frequency response characteristic about the centre frequency as (fig.3.16) as transmission zeros are not divided equally between the origin and the infinity. As the zeros are fixed by the assumption of double tuned configuration, symmetrical response was obtained by modifying the pole positions from their original locations.

Digital computer was used to determine the frequency response using the shifted poles and zeros, the result obtained closely matched the ideal Chebyshev bandpass response.

The parameters of each interstage network have been evaluated realizing the poles and zeros that have been assigned to it for realization. The complete circuit was constructed and its frequency response characteristic was plotted from the measurement.

The comparison of the ideal and measured responses shows that the measured response is quite satisfactory although the number of ripples is fewer in the measured response. As the separation between the peak positions of ripples is less, it is quite likely that peaks might have merged because the Q of coils were not too high and it is often difficult to measure the Q exactly at high frequency.

In case double tuned circuit, oscillations, resulting from the poles that are nearer to the imaginary axis, create some problem in the tuning process. The oscillation can be stopped by introducing some loss in the respective coils, but this will cause reduction in passband gain.

The response obtained using double tuned circuit is much better when compared with that of the single tuned circuit. For example, the three stage single tuned amplifier gives an attenuation of -8 db down at frequency 485 KHz from its value at the centre frequency $f_0 = 455$ KHz whereas the double tuned amplifier gives an attenuation of -21 db down at frequency 405 KHz.

4-37833

The result can further be improved by increasing the number of poles and zeros i.e. by increasing the number of stages or looking for other types of inter-stage networks. The interstage can also be synthesized increasing its complexity which may not improve the result, as some of the losses in inductors may not be possible to absorb in the networks as circuit elements. The zeros and poles can be realized by R-C network although its zeros and poles always lie along the real axis. A positive feedback in a transistor amplifier results oscillation which indicates that the zeros and poles now lie in the complex plane. Therefore, R-C networks which provide positive feedback in a transistor amplifier can be used to realize the zeros and poles of the over-all transfer function that achieve prescribed response and eliminates the troublesome inductors.

APPENDIX-A

MEASUREMENT OF h-PARAMETERS

Experimental Set-up for the Measurement of the h-parameter.

Measurement of h_{ie} and h_{fe}

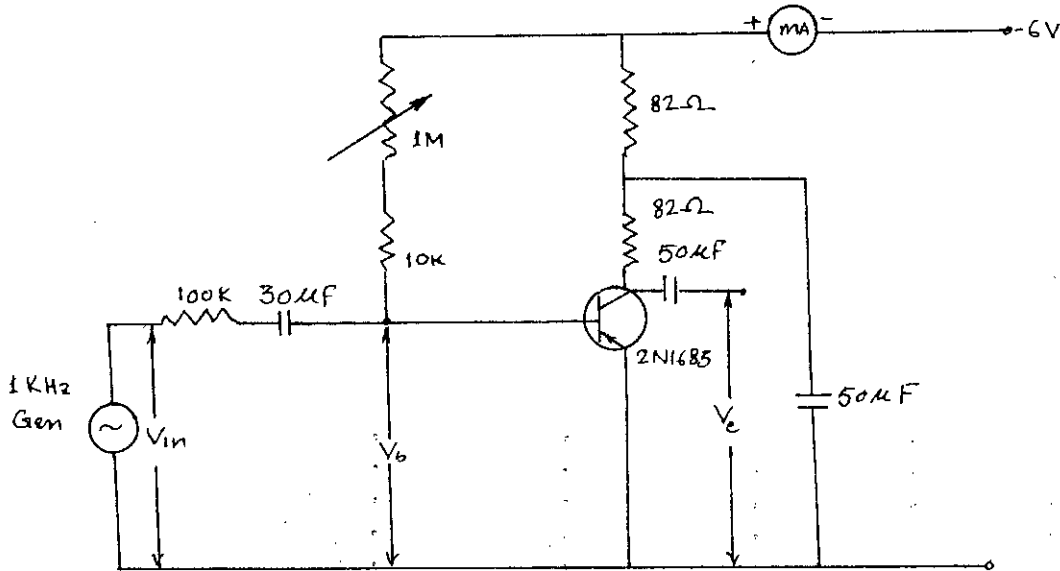


Figure A1.1.

A circuit was constructed as shown in fig.A1.1. D.C. collector current was set at 1 mA by 1M potentiometer. A signal generator set at 1Kc/s was applied to the terminals as shown in fig.A1.1. For various values of V_{in} (without disturbing the output V_c), V_b and V_c were measured and tabulated in table A1.1.

TABLE A1.1

For $I_c = 1 \text{ mA}$.

V_{in} in volts	V_b in 10^{-3}	V_c in volts	$I_b = V_{in}/10^5$ in amperes $\times 10^5$	$I_c = V_c/82$ in amperes $\times 10^{-4}$
0.10	1.90	0.0075	0.10	0.915
0.15	3.10	0.01	0.15	1.22
0.22	4.70	0.015	0.22	1.82
0.25	5.30	0.017	0.25	2.07
0.30	6.45	0.02	0.30	2.44
0.35	7.35	0.0225	0.35	2.74
0.38	8.2	0.025	0.38	3.05
0.40	8.6	0.0265	0.40	3.25

Determination of h_{ie}

The parameter h_{ie} is defined as the change in emitter-base voltage divided by the resulting change in base current, dc collector voltage being constant.

$$h_{ie} = \frac{\partial V_{be}}{\partial I_B} \bigg|_{V_c} = \frac{V_b}{I_b} \bigg|_{V_c=0}$$

As the 82Ω collector load is small compared with output impedance it may be ignored and output may be considered shorted to A.C. while the collector voltage is effectively constant. Also $100 k\Omega$ resistor in the base circuit is high compared with the transistor input impedance.

The plot of V_b , V_c , I_b from table A.1 is shown in fig. A.2. From the plot h_{ie} was calculated as

$$h_{ie} = \frac{V_b}{I_b} = \frac{8.45 \times 10^{-3}}{0.3 \times 10^{-5}} = 2.15 K$$

Determination of h_{fe}

This parameter is defined as the ratio of the change in the collector current to the change in the base current; the collector D.C. voltage being constant.

$$h_{fe} = \frac{I_c}{I_B} \bigg|_{V_c} = \frac{I_c}{I_b} \bigg|_{V_c=0}$$

The curve of I_c vs I_b (data from table A.1) is plotted in Fig. A.3. The curve h_{fe} calculated as

$$h_{fe} = \frac{I_c}{I_b} = \frac{3.23 \times 10^{-4}}{0.4 \times 10^{-5}} = 80.$$

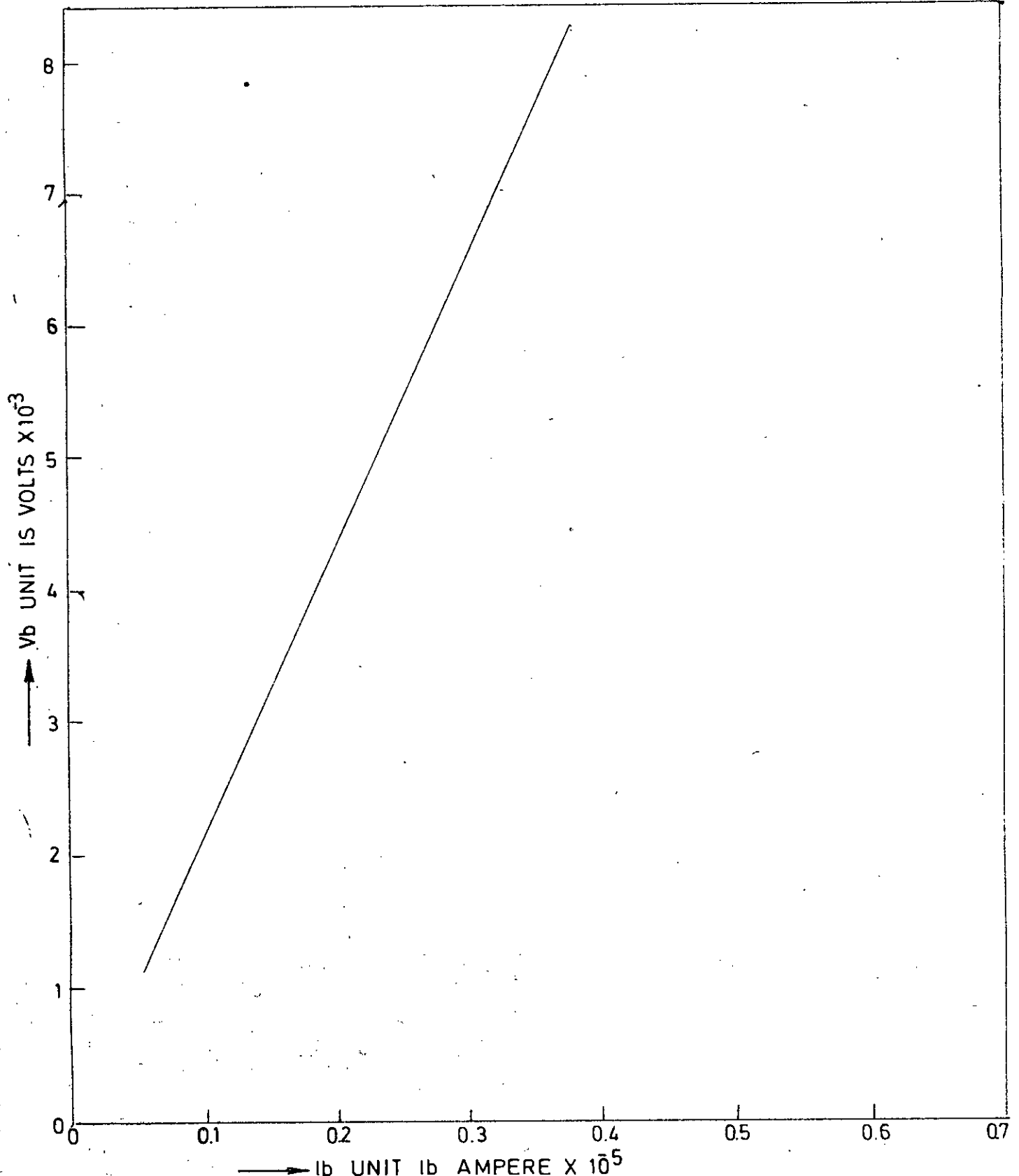


FIG. A.2 V_b VS. I_b CURVE TO CALCULATE h_{ie}

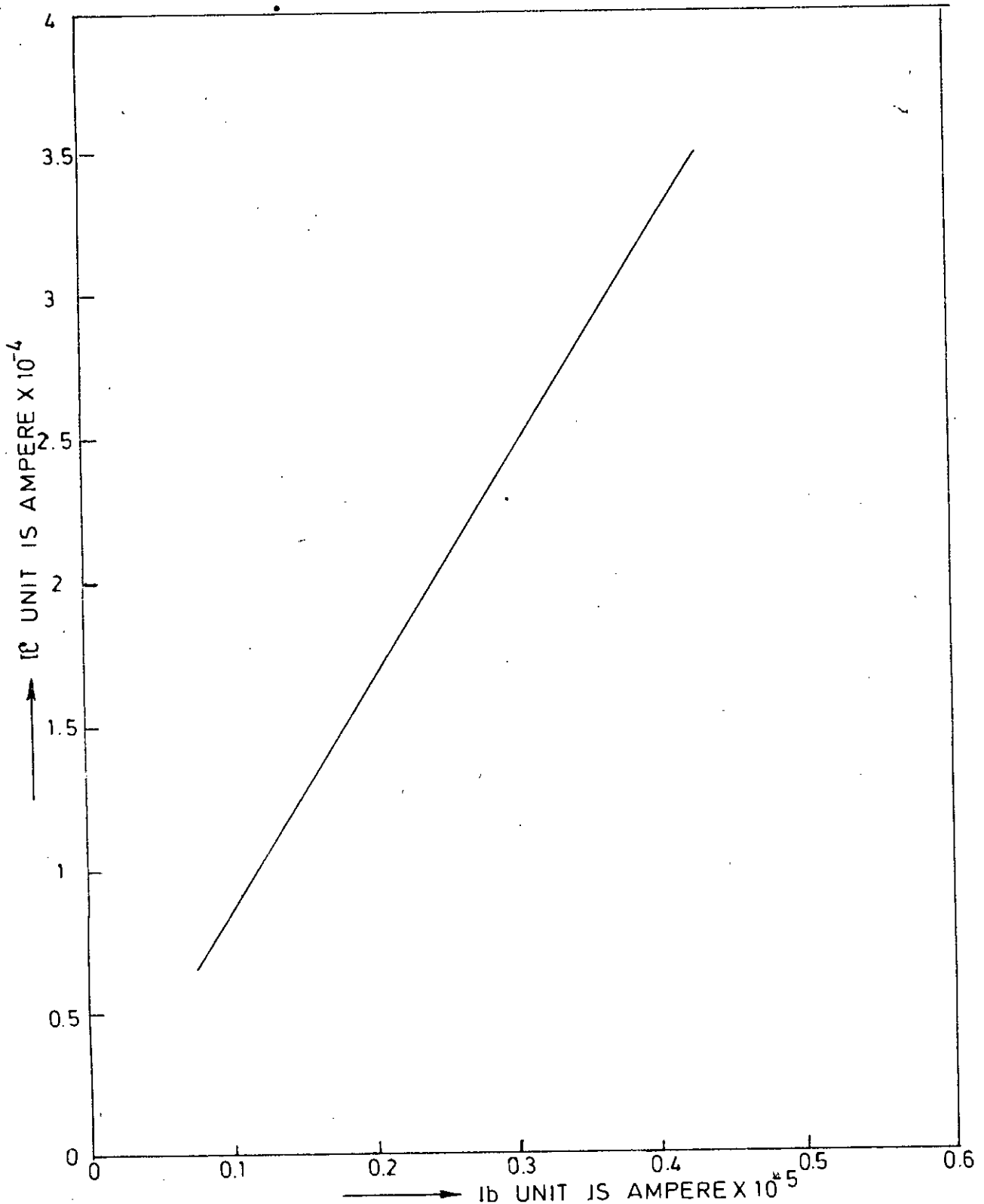


FIG. A.3 I_c VS I_b CURVE TO CALCULATE h_{fe}

Measurement of h_{re}

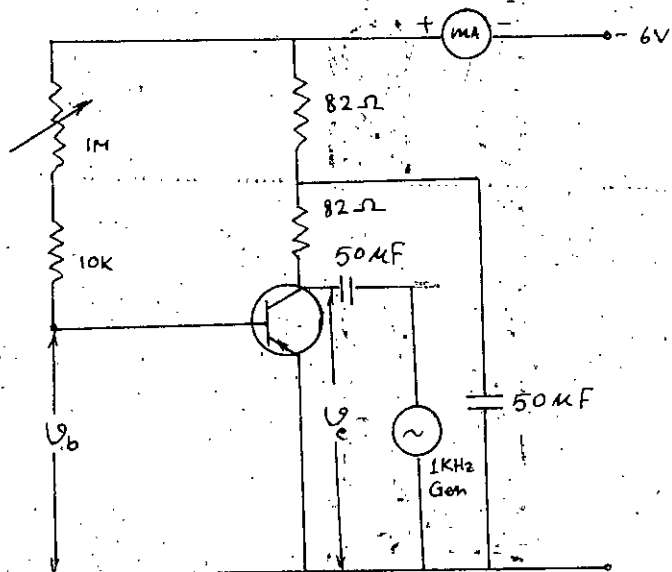


Fig. A.4.

A circuit was constructed as shown in fig. A.4. D.C. collector current was set by the potentiometer. A signal generator not at was applied to the terminals as shown in fig. A.4. For various values of V_c , V_b was measured and tabulated in table A.2.

Table A.2

For $I_c = 10\mu A$

V_b in volts	V_c in volts	V_b in volts $\times 10^{-4}$
0.20	0.020	0.52
0.30	0.039	1.01
0.40	0.054	1.40
0.50	0.065	1.70
0.80	0.10	2.6
0.90	0.125	3.24
1.00	0.145	3.75
1.30	0.18	4.66
1.50	0.20	5.20
1.80	0.24	6.22
2.00	0.27	7.00
2.30	0.30	7.77
2.50	0.33	8.50

* As V_b was small, it was measured by using an amplifier of Gain ≈ 385 .

Determination of h_{re}

This parameter is defined as the ratio of the change in the base-voltage to the change in the collector voltage, the base current being constant.

$$h_{re} = \frac{\partial V_b}{\partial V_c} \Big|_{i_b} = \frac{V_b}{V_c} \Big|_{i_b}$$

As the base resistor is high, the base current may be taken to be constant.

The curve of V_b vs V_c is plotted in fig. A.5 and h_{re} calculated as

$$h_{re} = \frac{V_b}{V_c} = \frac{3.36 \times 10^{-4}}{1} = 3.36 \times 10^{-4}$$

Measurement of h_{oe}

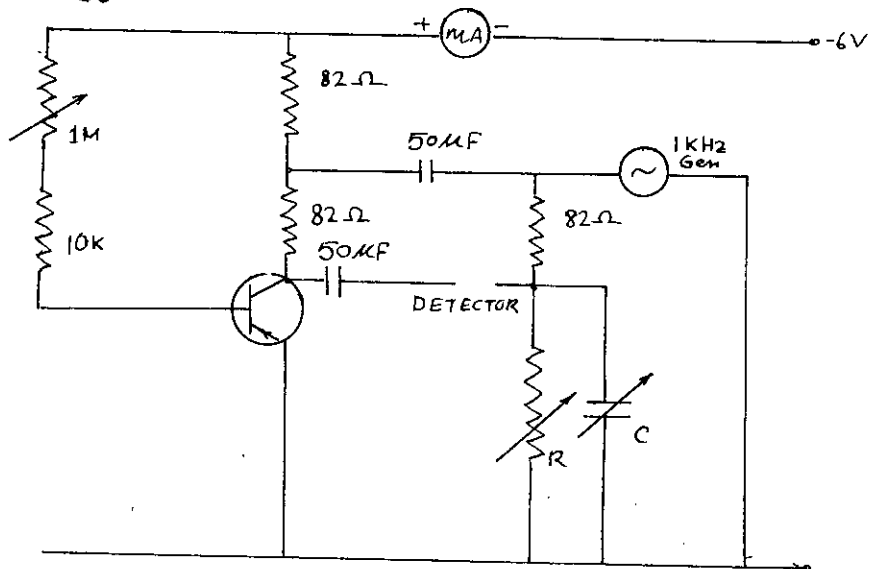


Fig. A.6

R - 100K decade Box.

C - 1000 pF Calibrated capacitor.

The circuit of fig. A.6 was constructed and d.c. was set at 1 mA. detector was oscilloscope. The bridge was balanced by varying the decade resistor R and calibrated capacitor C. The reading was

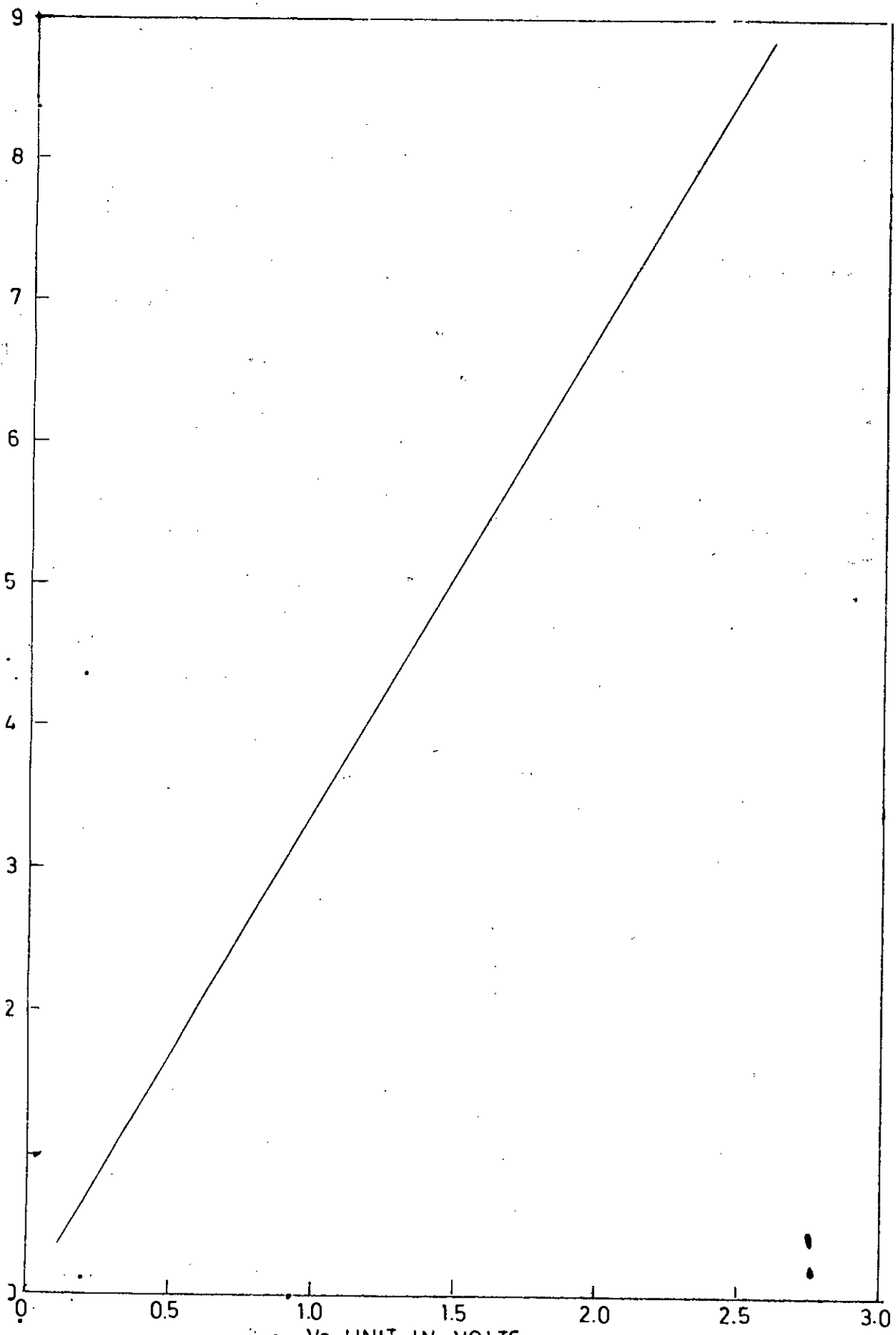


FIG. A 5 μh VS V_c CURVE TO CALCULATE hrc

$$R = 38.4 \text{ K}$$

$$h_{oe} = \frac{1}{R} = 2.6 \times 10^{-5} \text{ mho}$$

Hybrid- π Model

The hybrid- π model of a transistor at high frequency is shown in fig. A.7.

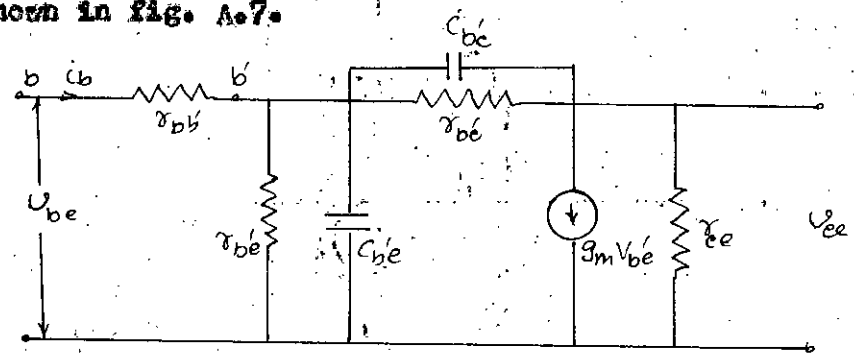


Fig. A.7 Hybrid- π Model.

where r_{bb} - base-spreading resistance, representing an average value of resistance of active and inactive region of the base.

$r_{b'c}$ - accounts for the increase in base current due to the widening of the base width for a decrease in collector voltage.

$r_{c'b'}$ - accounts for the decrease in collector current due to the widening of the base width for a decrease in collector voltage.

$C_{b'e}$ - represents the diffusion and transition capacitance in the emitter junction.

$C_{b'c}$ - represents the diffusion and transition capacitances in the collector junction.

Relation between h-parameters and hybrid-model elements.

To find h_{ie} , the voltage V_{ce} of Fig. A.7 is made zero by shorting the collector and emitter terminals and V_{be} due to an input current i_b becomes (capacitances are neglected and h_{ie} is considered resistive at low frequency).

$$V_{be} = i_b [r_{bb'} + r_{b'e} r_{b'c} / (r_{b'e} + r_{b'c})]$$

which gives

$$h_{ie} = r_{bb'} + \frac{r_{b'e}}{1 + r_{b'e} / r_{b'c}} \quad \text{.....(A.1)}$$

But $\frac{r_{b'e}}{r_{b'c}} \ll 1$. eqn. (A.1) becomes

$$h_{ie} = r_{bb'} + r_{b'e} \quad \text{.....(A.2)}$$

To find h_{fe} , we have the output shorted and calculate the short circuit current as

$$i_c = \beta_m V_{b'e} = \frac{\beta_m V_{b'e}}{r_{b'c}}$$

where $V_{b'e} = i_b [r_{b'e} r_{b'c} / (r_{b'e} + r_{b'c})]$ which gives

$$i_c = \frac{i_b}{1 + r_{b'e} / r_{b'c}} [\beta_m r_{b'e} = \frac{\beta_m r_{b'e}}{r_{b'c}}]$$

But

therefore, the forward short-circuit current gain becomes

$$h_{fe} = i_c / i_b = \beta_m r_{b'e} \quad \text{.....(A.3)}$$

To find h_{re} , the condition that i_b be zero implies that the output terminals be open-circuited. For an applied voltage V_{ce} ,

$$V_{be} = V_{ce} [r_{b'e} / (r_{b'e} + r_{b'c})] \quad \text{.....(A.4)}$$

which gives

$$h_{re} = V_{be} / V_{ce} = r_{b'e} / r_{b'c}$$

To find h_{oe} the input terminals remain open-circuited. For an applied voltage V_{ce}

$$i_c = V_{ce} \left[\frac{1}{r_{ce}} + \frac{1}{(r_{b'c} + r_{b'e})} + \beta_m \frac{V_{b'e}}{r_{b'e}} \right]$$

where $V_{b'e} = V_{ce} / (r_{be} + r_{b'e})$, which gives the collector current as

$$i_c = V_{ce} \left[\frac{1}{r_{ce}} + \beta_m \frac{r_{b'e}}{(r_{b'c} + r_{b'e})} \right]$$

and the output conductance becomes

$$h_{oe} = i_c / V_{ce} = \frac{1}{r_{ce}} + \beta_m \frac{r_{b'e}}{r_{b'c}} \tag{A.5}$$

But $r_{ce} = r_{b'c} / r_{b'e} \beta_m$, therefore eqn. (A.5) becomes

$$h_{oe} = \frac{1}{r_{ce}} + \frac{1}{r_{ce}} = \frac{2}{r_{ce}} \tag{A.6}$$

Determination of hybrid model parameters.

β_m is defined as

$$\beta_m = \frac{\Delta I_c}{\Delta V_{EB}} = \frac{q I_c}{K T} \tag{A.7}$$

where $K/q = .025$ v at $20^\circ C$

Having found h_{fe}

$$r_{b'e} = h_{fe} / \beta_m \tag{A.8}$$

with $r_{b'e}$ known $r_{bb'}$ can be found as

$$r_{bb'} = h_{ie} - r_{b'e} \tag{A.9}$$

with h_{re} known, $r_{b'c}$ can be found as

$$r_{b'c} = r_{b'e} / h_{re} \tag{A.10}$$

and r_{co} is calculated as

$$r_{co} = \frac{1}{h_{re} (\beta_m)} \tag{A.11}$$

Appendix-B

DETERMINATION OF BANDPASS POLES

C*****A. M. MAZUMDER, E.E. DEPARTMENT, M.SC. THESIS

C*****FREQUENCY TRANSFORMATION OF LOWPASS TO BANDPASS POLE

C*****R=REAL PART, AIM=IMAGINARY PART

```

N=5
102 DO 100 I=1,N
  READ(1,2)R,AIM
  2 FORMAT(2F10.5)
  E=0.5493
  Y=N
  A=(ALOG((1.0+((1.0+E**2)**0.5))/E))/Y
  D=TANH(A)
  R1=R*D
  AIM1=AIM
  WRITE(3,7)R1,AIM1
  7 FORMAT(2F15.5)
  P1=3.14159
  W1=2.*PI*435000.
  W2=2.*PI*475000.
  W0=(W1*W2)**0.5
  D=(W2-W1)/(2.*W0)
  Z=((1.-(D**2)*(R1**2-AIM1**2))**2+(2.*R1*AIM1*(D**2))**2)**0.25
  X=0.5*(ATAN((-2.*(D**2)*R1*AIM1)/(1.-(D**2)*(R1**2-AIM1**2))))
  G=2.*PI*1000000.
  R2=(W0*(D*R1-Z*SIN(X)))/G
  AIM2=(W0*(AIM1*D+Z*COS(X)))/G
  R3=(W0*(D*R1+Z*SIN(X)))/G
  AIM3=(W0*(AIM1*D-Z*COS(X)))/G
  WRITE(3,6)R2,AIM2,R3,AIM3
  6 FORMAT(4F10.5)
100 CONTINUE
103 CALL EXIT
  END
```


DETERMINATION OF THE FREQUENCY RESPONSE OF A CHEBYSHEV BANDPASS FILTER

```
C*****A.M.MAZUMDER, E.E.DEPARTMENT, M. SC. THESIS
C*****FREQUENCY RESPONSE OF A CHEBYSHEV ACTIVE BANDPASS FILTER
      DIMENSION PR(12),PI(12)
      READ(1,2)N,K
      2  FORMAT(2I5)
      4  FORMAT(6F10.5)
      READ(1,4)(PR(I),I=1,N),(PI(I),I=1,N)
      FR=.455
      NC=88
      DO 9 J=1,NC
      AR=1.0
      AI=0.0
      W=FR
      DO 17 I=1,N
      CR=AR*(-PR(I))- (W+(-PI(I)))*AI
      CI=AR*(W+(-PI(I)))+(-PR(I))*AI
      AR=CR
      AI=CI
      17 CONTINUE
      DR=-(W)**K
      X=(DR*AR)/(AR**2+AI**2)
      Y=(DR*AI)/(AR**2+AI**2)
      104 Z=(X**2+Y**2)**0.5
      IF(FR-0.455)20,21,20
      21 DFZ=Z
      DB=20.*ALOG10(BFZ)
      WRITE(3,7)FR,BFZ,DB
      7  FORMAT(3E15.5)
      FR=0.09
      GO TO 9
      20 Z=Z/BFZ
      DB=20.*ALOG10(Z)
      WRITE(3,7)FR,Z,DB
      IF(FR-0.4)10,11,11
      10 FR=FR+0.01
      GO TO 9
      11 IF(FR-0.49)12,12,13
      12 FR=FR+0.002
      GO TO 9
      13 IF(FR-0.6)10,10,50
      9  CONTINUE
      WRITE(3,32)
      32 FORMAT(//)
      50 CALL EXIT
      END
```

APPENDIX-D

DETERMINATION OF POLE LOCATIONS FOR SYMMETRICAL RESPONSE IN
DOUBLE TUNED NETWORK.

C*****A.M.MAZUMDER,E.E.DEPARTMENT, M.SC. THESIS
C*****POLE LOCATIONS FOR SYMMETRICAL FREQUENCY RESPONSE

```
DIMENSION PR(12),PI(12)
READ(1,2)N,K
2 FORMAT(3I5)
4 FORMAT(6F10.5)
READ(1,4)(PR(I),I=1,N),(PI(I),I=1,N)
NB=10
DO 100 L=1,NB
PR(1)=PR(1)-0.00002
PR(2)=PR(2)-0.00002
PR(3)=PR(3)+0.00002
PR(4)=PR(4)+0.00002
PR(5)=PR(5)-0.00002
PR(6)=PR(6)-0.00002
PR(7)=PR(7)+0.00002
PR(8)=PR(8)+0.00002
PR(9)=PR(9)-0.00002
PR(10)=PR(10)-0.00002
PR(11)=PR(11)+0.00002
PR(12)=PR(12)+0.00002
WRITE(3,6)(PR(I),I=1,N),(PI(I),I=1,N)
6 FORMAT(1H1,10X,6F10.5)
6 FR=0.455
NC=32
DO 9 J=1,NC
AR=1.0
AI=0.0
CR=AR*(-PR(I))- (W+(-PI(I)))*AI
CI=AR*(W+(-PI(I)))+(-PR(I))*AI
AR=CR
AI=CI
17 CONTINUE
DR=- (W)**K
X=(DR*AR)/(AR**2+AI**2)
Y=(DR*AI)/(AR**2+AI**2)
104 Z=(X**2+Y**2)**0.5
IF (FR-0.455)20,31,20
31 BFZ=Z
DB=2.*ALOG10(BFZ)
WRITE(3,7)PR,BFZ,DB
7 FORMAT(11X,3E15.5)
FR=0.426
GO TO 9
20 Z=Z/BFZ
DB=20.*ALOG10(Z)
WRITE(3,7)PR,Z,DB
```

APPENDIX-D

IF (FR-0.486) 12, 12, 100
12 FR=FR+0.002
9 CONTINUE
100 CONTINUE
50 CALL EXIT
END

APPENDIX-E

DETERMINATION OF THE PARAMETERS OF EACH INTERSTAGE OF THE
DOUBLE TUNED FILTER

```
C*****A.M.MAZUMDER,E.E.DEPARTMENT, M.SC. THESIS
C*****CALCULATIONS OF PARAMETERS
      DOUBLE PRECISION F1,F2
C*****X=R1/L1,Y=R2/L2,Z=1/(L1C1),W=1/(L2C2)
      DOUBLE PRECISION X,C1,C2,C3,C4,D,X1,Y,Z,P,P1,E1,E2,E3,E4,E5,E6
106 READ(1,100)C1,C2,C3,C4,D,X1
100 FORMAT(6D13.5)
      WRITE(3,100)C1,C2,C4,C3,D,X1
110 FORMAT(1H1,6D15.5)
      A1=C1*(10.**6)
      A2=C2*(10.**14)
      A3=C3*(10.**10)
      A4=C4*(10.**26)
      A5=1.0-D**2
      E1=A5*A1
      E2=A5*A2
      E3=A5*A3
      E4=A5*A4
      NB=300

      DO 102 L=1,NB
      X=X1*(10.**5)
      Y=E1-X
      E6=E2-X*Y
      Z=(E3-X*E6)/(Y-X)
      W=E6-Z
      P=Z*W
      F1=(Z**0.5)/(2.**3.14159)
      F2=(W**0.5)/(2.**3.14159)
      WRITE(3,104)X,Y,Z,W,P,E4,F1,F2
104 FORMAT(8D15.5)
      IF (P-E4)101,103,101
101 X1=X1+.001
102 CONTINUE
103 WRITE(3,105)X,Y,Z,W
105 FORMAT(1H1,4D15.5)
      GO TO 106
107 CALL EXIT
      END
```

REFERENCES

1. Grob, B., Basic Electronics, McGraw-Hill Book Company, Inc, New-York, 1959.
2. Fitchen, F.C., Transistor Circuit Analysis and Design, D. Van Nostrand Company, Inc., New-york, 1960.
3. Read, M.G., Electric Network Synthesis, Prentice-Hall, New-york, 1955.
4. Zverev, A.I., Handbook of Filter Synthesis, John Wiley & Sons, Inc, New-york, 1967.
5. Van Valkenburg, H.E., Introduction to Modern Network Synthesis, John Wiley & Sons, Inc., New york, 1960.
6. Ghansi, M.S., Principles and Design of Linear Active Circuits, Tata McGraw-Hill Publishing Company Ltd., Bombay-New Delhi, 1965.
7. Searle, C.L., Elementary Circuit Properties of Transistors, SEEC Vol.3, Boothroyd, A.R., John Wiley & Sons, Inc, New York, 1964.
8. Winkler, S., "The Approximation Problem of Network Synthesis", Trans. IRE, CT-1, No.3, Sept., PP 5-20, 1954.
9. Weinberg, L., Network Analysis and Synthesis, McGraw-Hill Book Company, Inc., New York, 1962.
10. Papoulis, A., "On the approximation Problem in Filter Design", IRE Natl. Conv. Record, Vol.5, Pt.2, PP 175-185, 1957.
11. Cochran, B.L., Transistor Circuit Engineering, The Macmillan Company, New York, 1967.
12. Angelo, E.J., Electronic Circuits, McGraw-Hill Book Company, Inc., New York, 1958.
13. Guillemin, E.A., Synthesis of Passive Networks, John Wiley & Sons, Inc., New York, 1957.
14. Tuttle, Jr. D.F., Network Synthesis, Vol.1, John Wiley & Sons, Inc., New York, 1958.
15. Stewart, J.L., Circuit Theory and Design, John Wiley & Sons, Inc., New York, 1956.

T-46

